Construction and Building Materials 443 (2024) 137700

Contents lists available at ScienceDirect

Construction and Building Materials

journal homepage: www.elsevier.com/locate/conbuildmat

Cyclic response and stability of shape memory alloy cables considering training, displacement history, and prestrain effects

Fei Shi [a], Malik Corum [b], Osman E. Ozbulut [b,c,*]

[a] School of Physics and Materials Science, Guangzhou University, Guangzhou, Guangdong Province, China
[b] Department of Civil and Environmental Engineering, University of Virginia, Charlottesville, VA, USA
[c] School of Civil Engineering, University of Leeds, Leeds, UK

ARTICLE INFO

Keywords:
Shape memory alloy
Cyclic stability
Strength degradation
Training cycles

ABSTRACT

Superelastic shape memory alloy (SMA) cables have been considered in the development of various seismic protection technologies. The cyclic nature of seismic loads necessitates a comprehensive understanding of the mechanical behavior of SMA cables under repeated loading conditions. As SMAs undergo repeated phase transformation cycles, alterations in their properties occur due to defects generated and modified during the transformation. When utilizing superelasticity, this response can be stabilized after numerous transformation cycles. In various applications, components made of SMAs undergo a stabilization process referred to as training to enhance the predictability of the alloy's response. Despite the widespread acceptance of training cycles to achieve stable cyclic response, a well-defined protocol is lacking. This study investigates the effects of various factors, including training strain amplitude, repeated loading, low-cycle fatigue loading, loading at high strain amplitudes, displacement loading history, and prestrain on the cyclic response of a large-diameter SMA cable. A total of 14 SMA cable specimens are tested under various tensile loading conditions. The experimental results, including stress-strain curves and various response parameters such as peak stress, residual strains, energy dissipation capacity, and equivalent viscous damping are examined in detail. The results indicate that training SMA cables at a strain amplitude near the end of phase transformation plateau leads to a highly stable cyclic response. However, it is worth noting that, in comparison to untrained cables, training induces a softening effect in the cable response.

1. Introduction

Shape memory alloys (SMAs) are metallic alloys that can recover their initial shape through either temperature-induced (shape memory effect) or stress-induced (superelasticity) martensitic phase transformations. Both shape memory effect and superplastic SMAs exhibit unique characteristics, making them applicable in various fields, including biomedical, aerospace, and mechanical engineering. The Nickel-Titanium (NiTi) alloy is the most common type of SMA currently used in industry due to its high strength, high corrosion resistance, large damping capacity, good fatigue resistance and ability to recover large deformations [1].

Over the past two decades, superelastic NiTi SMAs have been investigated for seismic response control of civil structures [2,3]. The remarkable self-centering ability and energy dissipation capacity of superelastic SMAs hold great potential for mitigating earthquake response of structural systems [3]. As a result, various SMA-based seismic control technologies, including bracing systems [4–10], damping devices [11–16], and isolation devices [17–24] have been proposed. In these devices, various forms of SMAs including wire, bar, cable, and spring have been considered. Among them, the cable form of SMAs, which consists of individual wires or strands braided to create a large tensile force carrying member, has been studied by several researchers [25–30].

Given the cyclic nature of seismic loads, it becomes critical to characterize the behavior of SMAs under repeated loading conditions. It is well-established that the mechanical response of NiTi SMAs is sensitive to cyclic loading [31–36]. The superelastic characteristics, such as critical phase transformation stress levels, residual strains, and hysteresis loop size, degrades with increasing loading cycles, leading to what is known as "functional fatigue". Functional fatigue arise from strain incompatibility between the austenite and martensite phases, resulting in

* Corresponding author at: Department of Civil and Environmental Engineering, University of Virginia, Charlottesville, VA, USA.
E-mail address: ozbulut@virginia.edu (O.E. Ozbulut).

https://doi.org/10.1016/j.conbuildmat.2024.137700
Received 7 February 2024; Received in revised form 4 June 2024; Accepted 30 July 2024
Available online 5 August 2024

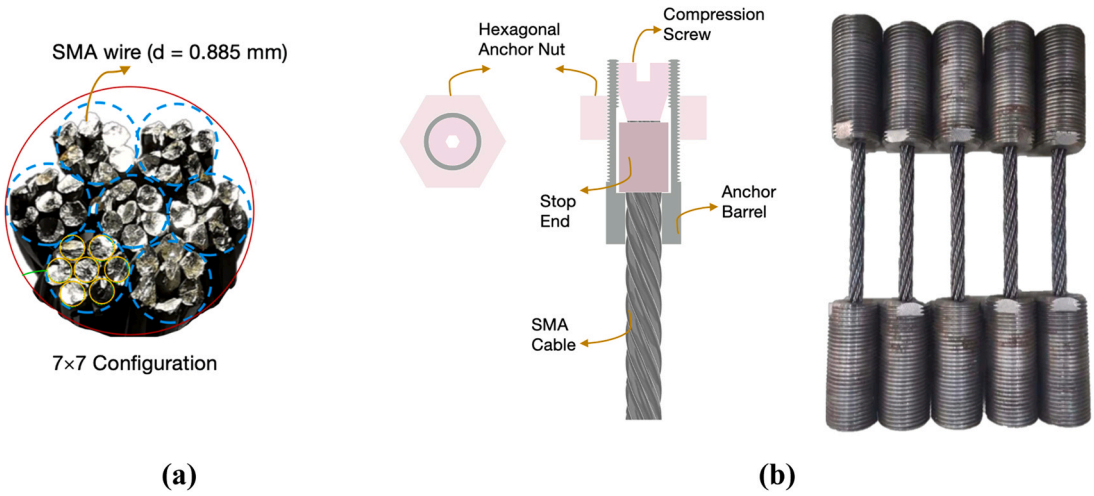

Fig. 1. (a) SMA cable configuration and (b) its anchorage system and test specimens.

the formation of localized stress concentrations and the generation of dislocations at the interfaces of these phases [37]. In addition to new dislocations that may occur due to mechanical loading, existing dislocations in the SMAs could also be activated during deformation [38]. All these dislocations contribute the formation of residual martensite and associated residual strains during unloading. This behavior is referred to as transformation induced plasticity (TRIP), as plastic deformations occur even when the applied stress levels are lower than the plastic yield strength [39]. However, during cyclic loading, the formation of residual martensite formation saturates when the local stresses cannot induce new dislocation slips, resulting in a more stabilized response after a certain number of loading cycles.

When using SMAs in seismic applications, it is important to understand and account for the variations in their mechanical properties under cyclic loading. To achieve stable mechanical behavior and reduce the functional fatigue, various researchers have proposed a training loading procedure for SMAs. Training involves subjecting SMAs a series of controlled mechanical deformations to optimize and enhance their mechanical properties. Experiments conducted by Ran et al. [40] revealed that the stability of forward and reverse transformation stresses can be improved significantly by constant cyclic training. Davarnia et al. [41] found that adding training loading cycles causes the loading plateau, unloading plateau and residual strains in SMA wires to approach stable levels within a small number of testing cycles. Wolons et al. [36] concluded that a considerable amount of mechanical preload cycling is required for an SMA wire to achieve a stable hysteresis loop shape.

Although the application of training cycles for a stable response is widely accepted, there is no clear guidance on the adopted training protocol [41]. Different strain/stress amplitudes and numbers of loading cycles have been selected in previous studies. For instance, Xia et al. [42] implemented a displacement-controlled training procedure of 20 cycles at 4 % strain while studying fatigue life. Zhang et al. [43] used a stress-controlled training protocol of 20 loading cycles at three stress levels to assess the effects mechanical training on the low cycle fatigue of SMAs. They found that increasing the training stress level improves fatigue lifetime. Soul et al. [32] applied a training at 8 % strain for 100 cycles to minimize appreciable changes in stress levels and accumulated residual strains in SMAs. Ozbulut et al. [34] used a training test procedure consisting of 20 loads cycles at 5 % strain loading while studying the effects of temperature on the response of SMAs. McCormick et al. [44] considered training of SMA wires at 3 % and 5 % strain for either 20 cycles or 60 cycles to obtain a stable mechanical behavior. Dolce and Cardone [45] examined the cyclic behavior of SMA wires for seismic applications and employed 10 training cycles at 7 % strain amplitude to stabilize the superelastic behavior of SMAs.

It is evident that there is absence of a well-defined training loading protocol for superelastic SMAs, especially for SMA cables. Furthermore, since earthquake loading is highly random, SMAs can be subjected to a high amplitude loading followed by moderate-to-low amplitude loading cycles in seismic applications. The application of a certain prestrain on SMAs is also considered when SMA wires or cables are used to fabricate seismic control devices. It was shown that the application of prestrain on SMAs can improve the initial stiffness [29] and energy dissipation capacity [46,47] of SMA-based seismic control devices. Therefore, it is important to understand the effects of displacement loading history and prestrain on the cyclic response of superelastic SMAs as well as their response beyond superelastic strain limits. To address these research gaps, this study investigates the effects of various factors such as training strain amplitude, repeated loading, displacement history, and prestrain on the cyclic response of a large-diameter SMA cable.

The extensive experimental tests conducted in this study provide data to help establishing an optimal training regime that effectively minimizes cyclic degradation and increases reliability and predictability of SMA cables when subjected to cyclic loading. First, the details on the SMA cable specimens, the experimental test setup, loading protocol and the test matrix used to characterize the cyclic stability of the cable specimens are introduced. Then, experimental results obtained through tensile testing are presented. Along with the stress-strain curves of specimens, the various parameters such as peak stress, residual strains, energy dissipation capacity, and equivalent viscous damping are analyzed and discussed next. Finally, the key findings of this study are summarized.

2. Experimental program

2.1. Materials and specimens

The SMA cables employed in this research are obtained from Fort Wayne Metals, and designed with a $7 \times 7 \times 0.885$ mm configuration. As shown in Fig. 1(a), the SMA cable is a built-up structure that consists of seven strands, and the outer six strands are wound around the core strand by using right-handed helix. Each strand has seven wires wrapped in a left-handed helix form. Each wire has a diameter of 0.885 mm with a black oxide surface finish, supplying an approximately outer SMA cable diameter of 8 mm and a cross-sectional area of 30.13 mm^2.

The NiTi wires are superelastic at room temperature with an austenite finish temperature of 19°C. The chemical composition of the SMA material consists of 56 % Nickel balanced with Ti. The elastic modulus of the cable is reported as 26.8 GPa by the manufacturer. A

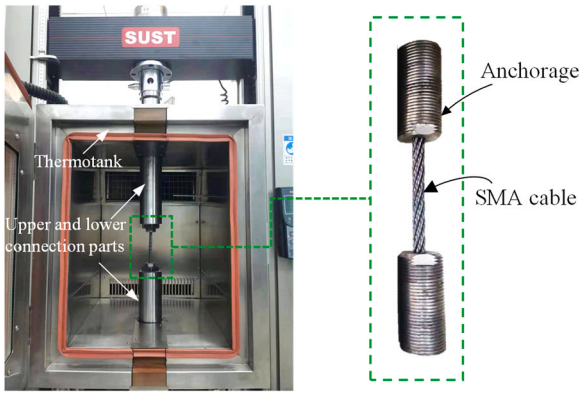

Fig. 2. Experimental test set up.

total of 14 SMA cable specimens are prepared for the tensile cyclic test. The ends of the SMA cables are fixed by utilizing a stop-end type anchorage system [48], which consists of anchor barrel, stop end and compression screw, as shown in Fig. 1(b). Both ends of the SMA cable are securely anchored prior to the tensile test.

2.2. Test Set Up

A SUST universal testing machine with a maximum 50 kN load capacity is employed for the cyclic tensile test as shown in Fig. 2. The force and displacement are recorded by the built-in sensors of the loading frame. The SMA cable specimen is connected to the loading frame by screwing the anchorage into the upper and lower connection parts. An additional hexagonal nut is designed to avoid the loosening between the connection parts and anchorage system during the test. All experimental testing are conducted at room temperature (20 °C) using a displacement-controlled testing protocol. A loading rate of 1 mm/min is applied during all tests.

2.3. Experimental Program

Table 1 outlines the loading protocol for the fourteen SMA cable specimens subjected to tensile testing during this study. The experimental program is designed to characterize the cyclic response and stability of SMA cables across five different loading series. Each series of experiments investigates the impact of various parameters on the cyclic response of the SMA cable.

In Series I testing, which involves four specimens, the focus is on exploring how training regimes at different strain amplitudes affect the cyclic stability of the cable. Specimen S1 is subject to testing without any training cycles, while specimens S2, S3, and S4 are subject to 30 training loading cycles at 4 %, 5 %, and 6 % strain, respectively. Both untrained and trained specimens are then tested at increasing strain amplitudes from 1 % to 6 %, with 1 % increments. Following this initial testing, the specimens are released from the loading frame and tested again under the same increasing strain amplitude loading protocol to evaluate the reproducibility of response during a second loading of the same SMA cables.

Series II testing examines cyclic stability at strain amplitude beyond superelastic strain limits. This series, comprising specimens S5 and S6, includes one specimen with training and one without, subjected to three loading cycles at strain amplitudes ranging from 7 % to 14 %, with 1 % increments. Series III testing focuses on cyclic stability at constant strain amplitudes for a low-cycle fatigue loading. Specimens S7 to S9 are first trained at 6 % for 30 loading cycles and then subjected to 31 loading cycles at constant strain amplitudes of 4 %, 5 % and 6 %, respectively.

Series IV testing explores the effect of displacement history on cyclic stability of the SMA cable specimens. Three specimens (S10, S11, and S12) are initially loaded for three cycles at high strain amplitudes of 6 %, 8 % and 10 %, respectively. Subsequently, the specimens undergo three loading cycles at strain amplitudes increasing from 1 % to 6 %. Finally, Series V testing examines the effect of prestraining on the response of SMA cable specimens. After being trained at 6 % for 30 loading cycles, the first specimen in the test (S13) is prestrained at 1 % strain and loaded at three cycles at strain amplitudes ranging from 2 % to 6 %. The

Table 1
Test matrix for characterization on cyclic stability of SMA cable.

Test objective	Cable Specimen	Effective length (mm)	Training cycle (strain)	Prestrain (%)	Loading strain (%)	Loading velocity (mm/min)	Loading cycle
Training effects and stability during increasing loading amplitude	S1	123	0	0	1, 2, 3, 4, 5, 6 –Release– (1 hour) 1, 2, 3, 4, 5, 6	1	3
	S2	121	30 (4 %)	0	1, 2, 3, 4, 5, 6 –Release– (1 hour) 1, 2, 3, 4, 5, 6	1	3
	S3	123	30 (5 %)	0	1, 2, 3, 4, 5, 6 –Release– (1 hour) 1, 2, 3, 4, 5, 6	1	3
	S4	123	30 (6 %)	0	1, 2, 3, 4, 5, 6 –Release– (1 hour) 1, 2, 3, 4, 5, 6	1	3
Cyclic response and stability at higher strain amplitude	S5	118	0	0	7, 8, 9, 10, 11, 12, 13, 14	1	3
	S6	120.6	30 (6 %)	0	7, 8, 9, 10, 11, 12, 13, 14	1	3
Cyclic stability at constant strain amplitude	S7	117.7	30 (6 %)	0	4	1	31
	S8	116.3	30 (6 %)	0	5	1	31
	S9	119	30 (6 %)	0	6	1	31
Effect of displacement history on cyclic response and stability	S10	122	3 (6 %)	0	1, 2, 3, 4, 5, 6	1	3
	S11	124	3 (8 %)	0	1, 2, 3, 4, 5, 6	1	3
	S12	120	3 (10 %)	0	1, 2, 3, 4, 5, 6	1	3
Effect of prestrain on cyclic response and stability	S13	117.2	30 (6 %)	1	2, 3, 4, 5, 6 –Release– 2, 3, 4, 5, 6	1	3
	S14	118.3	30 (6 %)	2	3, 4, 5, 6 –Release– 3, 4, 5, 6	1	3

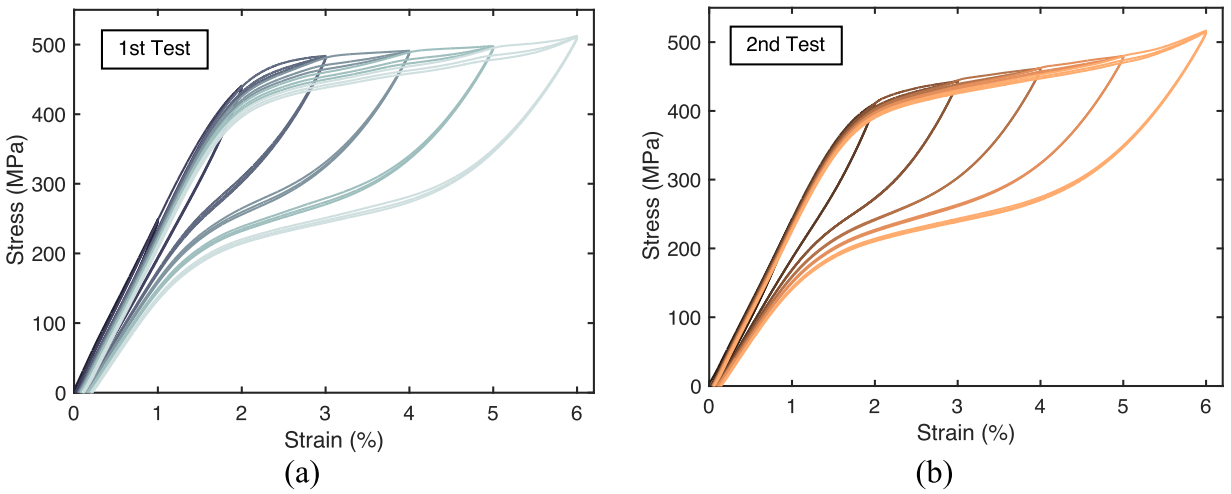

Fig. 3. Stress-strain curves of untrained SMA cable during (a) 1st and (b) 2nd tests.

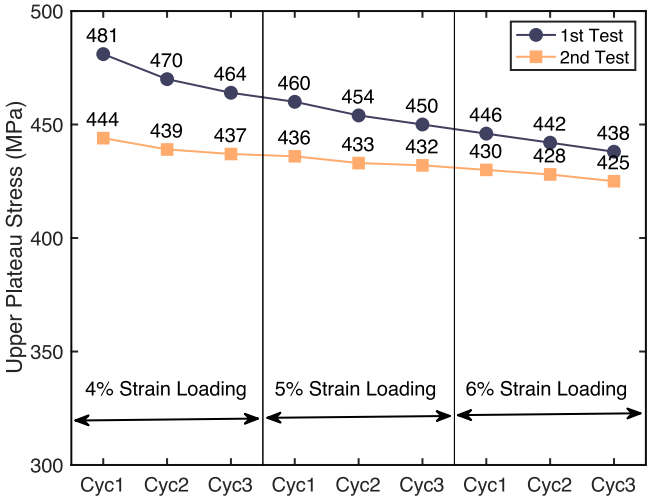

Fig. 4. Variation of UPS for untrained SMA cable during cyclic loading at 4 %, 5 %, and 6 % strain amplitudes.

specimen S14 is prestrained at 2 % strain and loaded at three cycles at strain amplitudes ranging from 3 % to 6 % strain.

3. Experimental Results

In this section, the results obtained from the testing of SMA cables under various loading conditions are presented. Parameters of interest, which includes second stiffness, dissipated energy, equivalent viscous damping ratio of the specimen, are calculated and analyzed for each specimen. The secant stiffness for each test is calculated by dividing the maximum force in the cable specimen by maximum displacement of the specimen. Dissipated strain energy quantifies the amount of energy dissipated during each loading cycle and is determined by calculating the area under the force-deformation curves of the analyzed test specimen. Equivalent viscous damping is a coefficient that represents the energy dissipated by the material due to its hysteric behavior and can be calculated using Eq. 1, where E_D is the energy dissipated and E_{SO} is the strain energy in the specimen. Additionally, the upper plateau stress (UPS), defined as the stress at 3 % strain during the loading of the specimen, is calculated and presented for some of the tested specimens.

$$\xi = \frac{1}{2\pi}\frac{E_D}{E_{so}} \tag{1}$$

3.1. Effects of training strain amplitude on cyclic stability

The effects of training strain amplitude on the cyclic stability of SMA cable specimens are examined through tensile testing of specimens S1 to S4 under an incrementally increasing strain amplitude loading protocol. At each strain amplitude, the specimens are subjected to three loading-unloading cycles. Note that the specimens are subjected to the same loading protocol twice, and the corresponding results are denoted as '1st Test' and '2nd Test' in the subsequent plots.

Fig. 3 shows the stress-strain curves of the untrained specimen S1 during the first and second tests for three loading-unloading cycles at all strain amplitudes. There is a downward shift in the loading plateau as the testing progresses to higher strain amplitudes during the first test. A more stabilized response is observed during the second test. This could be attributed to the possibility that the first test might have served as the training loading cycles.

In Fig. 4, the variation of UPS is presented for the SMA cable response under 4 %, 5 %, and 6 % strain loadings. In the first test, the UPS decreases from 481 MPa at the first cycle with a 4 % strain loading to 438 MPa at the third cycle with a 6 % strain loading, indicating a 9 % reduction in strength. During the second test, a similar decrease is observed under increasing strain amplitude testing, but the rate of this decrease is considerably smaller compared to the first test. In particular, there is only a 4 % decrease in the UPS between the first cycle with 4 % loading and third cycle with 6 % loading.

To facilitate a more straightforward comparison of responses among different loading cycles, Fig. 5(a) shows the first and third loading cycle responses for the first and second tests at strain amplitudes of 4 %, 5 % and 6 %. The results illustrate a slight downward shift in the loading response curve during the first and third loading cycles of the first test. In contrast, during the second test, the difference in the response obtained for loading cycles 1 and 3 is considerably small. When comparing the responses during the first test and second test, a more noticeable downward shift in the response is evident for the first test. Furthermore, a larger strength degradation is identified for 4 % strain amplitude loading compared to 5 % and 6 % strain loadings.

In Fig. 5(b), the variation in mechanical properties of SMA cable computed for the first loading cycle during the first and second tests is compared. The results indicate a slightly lower secant stiffness at 4 % and 5 % strain amplitude loading for the second test, while the dissipated energy remains almost the same for both tests. Consequently, a somewhat higher equivalent viscous damping is observed for the second test. On the other hand, for 6 % strain amplitude loading during the second test, the response of SMA cable exhibits a slight hardening behavior, resulting in a similar second stiffness (or maximum stress)

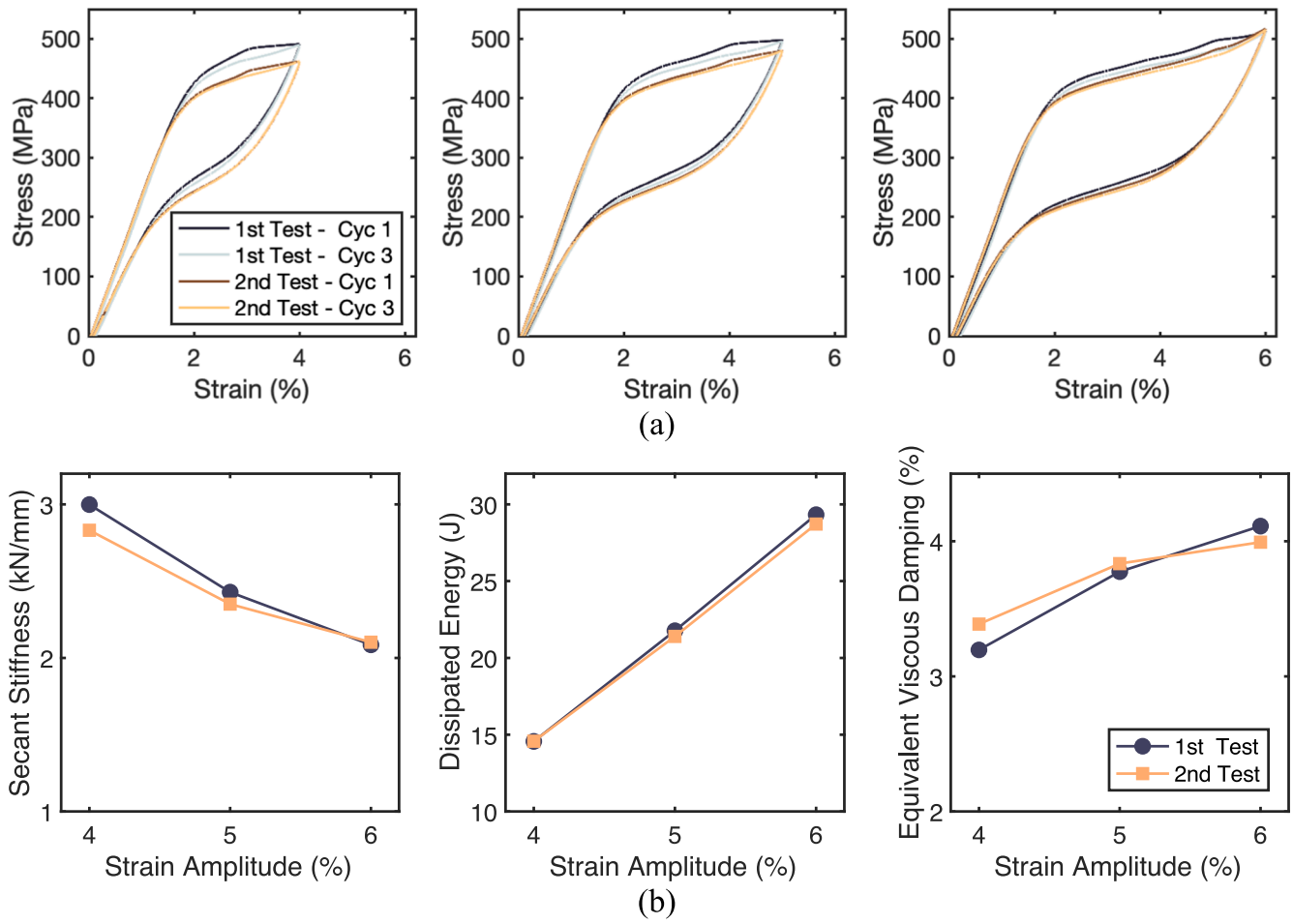

Fig. 5. (a) Hysteresis curves at cycle 1 and cycle 3 for untrained SMA cable and (b) variation of cyclic properties with strain amplitude during 1st and 2nd tests.

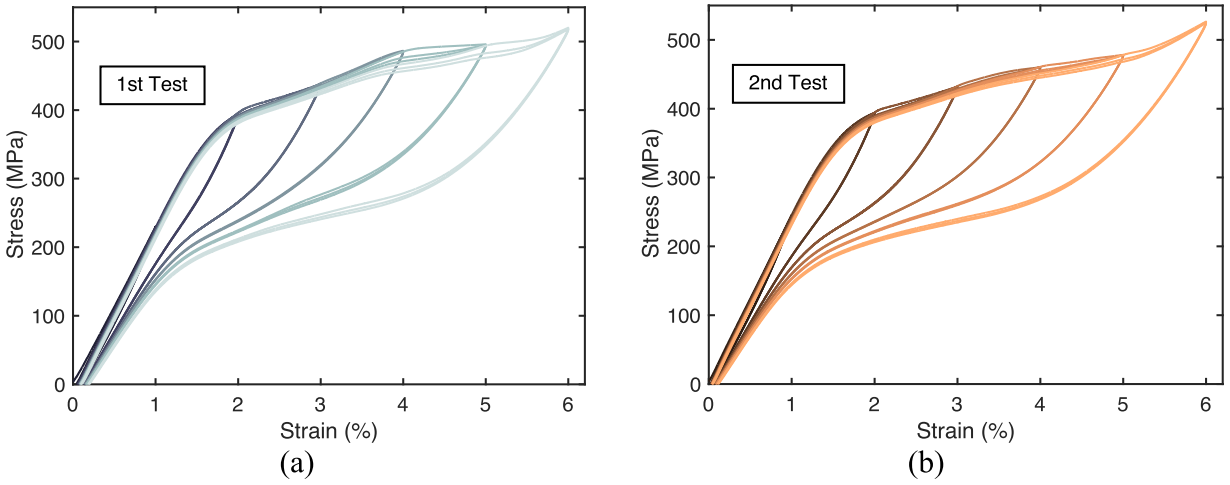

Fig. 6. Stress-strain curves of SMA cable trained at 4 % strain during (a) 1st and (b) 2nd tests.

with that of first test, while showing a slight decrease in both energy dissipation and equivalent viscous damping.

Fig. 6 shows the stress-strain response of specimen S2, which underwent training at 4 % strain for 30 cycles before being subjected to the specified loading protocol. The cyclic response at each strain amplitude appears more stable compared to the response of the specimen S1, which had no training cycles (Fig. 3). Although, there is still some degradation in the response, particularly during the first test, this degradation is smaller. As shown in Fig. 7, the UPS decreases from 439 at cycle 1 of 4 % loading to 423 MPa at cycle 3 of 6 % loading during the first test. This suggests a 3.6 % decrease in the UPS. The same decrease is 3.2 % during the second test.

Fig. 8(a) compares the stress-strain curves at 4 %, 5 %, and 6 % strain loadings for cycles 1 and 3 of the first and second tests. During the first test, the response of SMA cable at 4 % strain loading is almost identical for cycle 1 and 3. However, at 5 % and 6 % strain loadings,

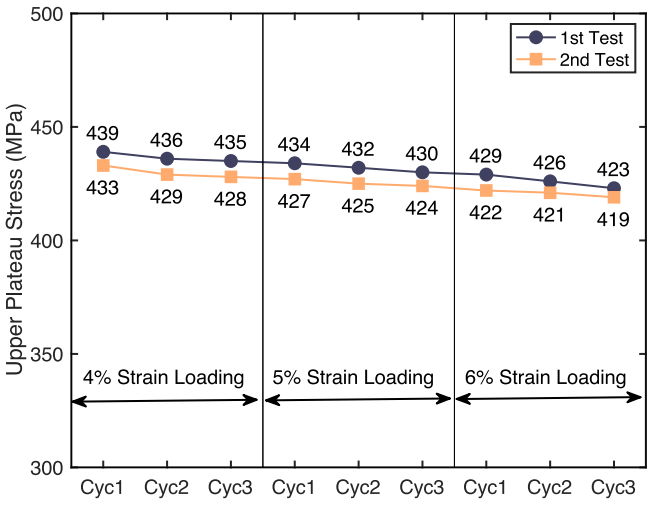

Fig. 7. Variation of UPS for SMA cable trained at 4 % strain during cyclic loading at 4 %, 5 %, and 6 % strain amplitudes.

there are some differences between cycle 1 and 3 of first test. This suggest that the SMA behavior stabilizes up to the strain amplitude at which training is conducted, i.e., 4 %, but it still has some variations at higher strain amplitude loadings. In addition, there is a clearer difference between the response curves of the first and second tests. This distinction is also evident in Fig. 8(b), where the variation of mechanical properties during the first and second tests is plotted. It is important to note that during the second test, the results are more stable at all displacement amplitude loadings. This increased stability during the second test is attributed to the applied loading cycles to the cable during the first test, as mentioned earlier.

Fig. 9 displays the stress-strain curves for specimen S3 which is trained at 5 % strain for 30 cycles before undergoing the applied loading protocol, while Fig. 10 shows the variation in the UPS for the same specimen. In contrast to prior test specimens, this specimen exhibits only slight variation in response under increasing amplitude loading and unloading cycles during the first and second tests. The decrease in the UPS is 2.8 % and 2.6 % from cycle 1 of 4 % loading to cycle 3 of 6 % loading during the first and the second tests, respectively. During cycle 1 and cycle 3 of 4 % and 5 % loading of the first test, there is almost no difference in the response, while there is some difference in the cyclic response for the 6 % loading as shown in Fig. 11(a). Compared to specimens S1 and S2, specimen S3 also has less degradation during the first and second tests, as evident from the response curves and the variation of mechanical properties shown in Fig. 11(b). These trends suggest that the increasing training amplitude correlates to a more stable cyclic curve.

Fig. 12 shows the stress-strain curves of specimen S4, which is traied at 6 % strain for 30 cycles. Minimal degradation is observed throughout the loading cycles at each strain amplitude, as well as between the first test and second test. As shown in Fig. 13, during both the first and

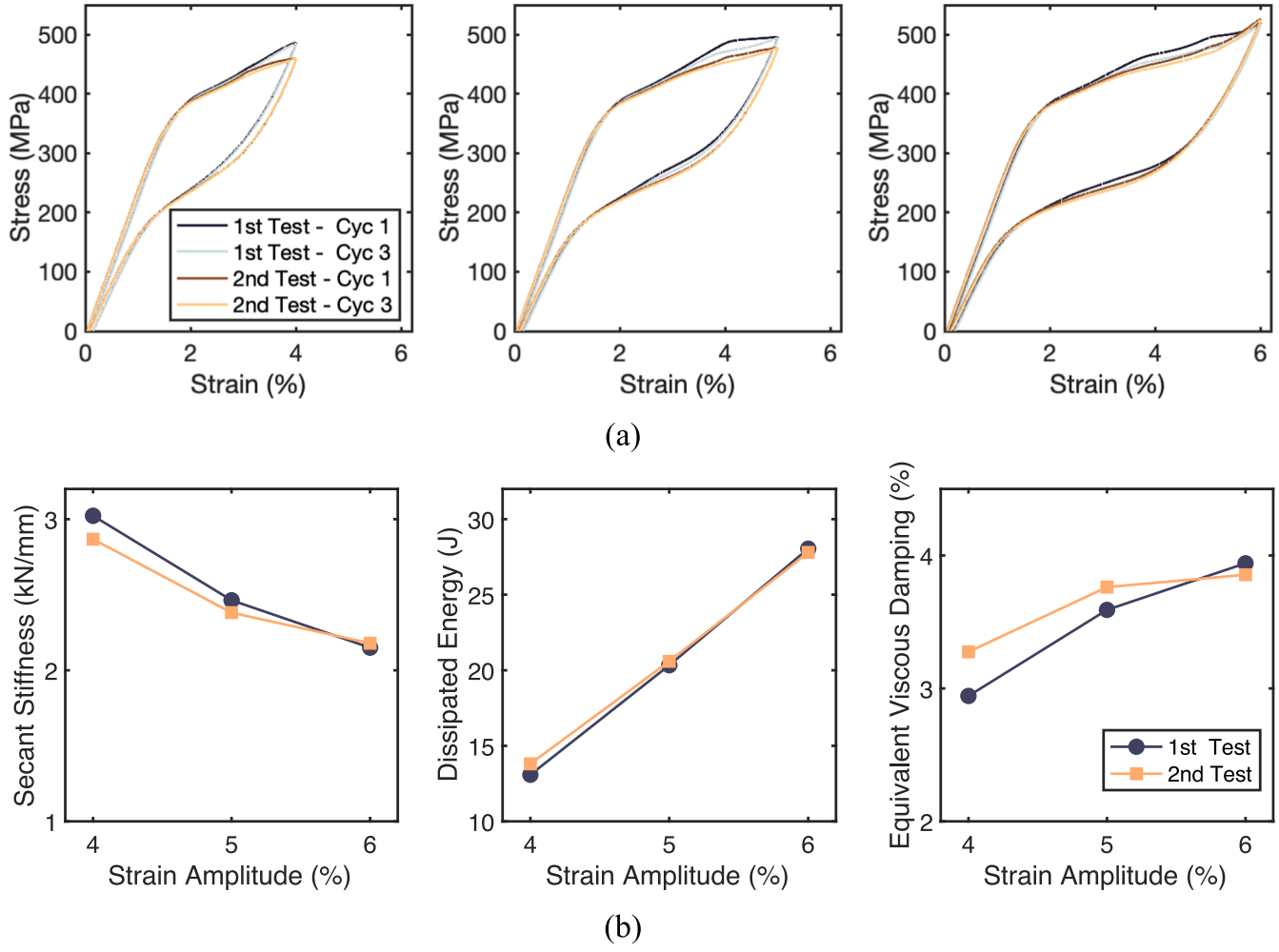

Fig. 8. (a) Hysteresis curves at cycle 1 and cycle 3 for SMA cable trained at 4 % strain and (b) variation of cyclic properties with strain amplitude during 1st and 2nd tests.

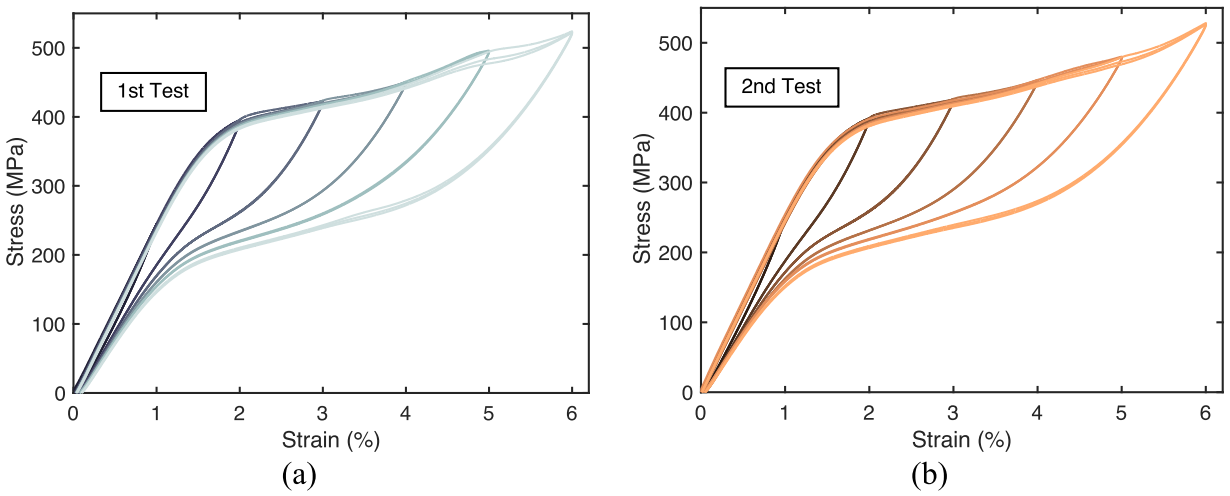

Fig. 9. Stress-strain curves of SMA cable trained at 5 % strain during (a) 1st and (b) 2nd tests.

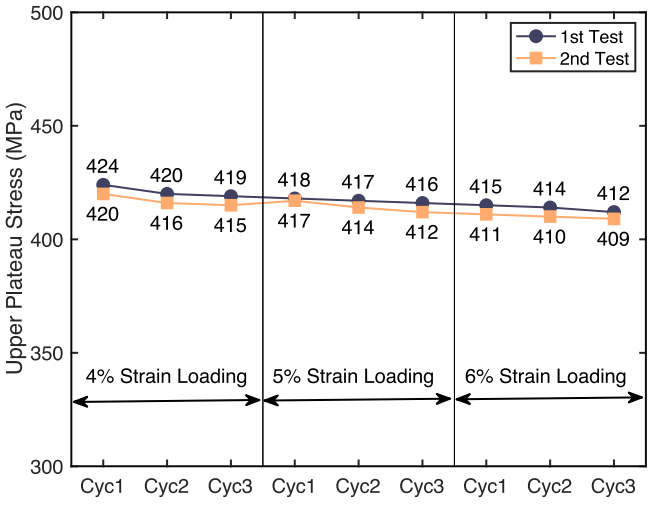

Fig. 10. Variation of UPS for SMA cable trained at 5 % strain during cyclic loading at 4 %, 5 %, and 6 % strain amplitudes.

second tests, the UPS decreases only 2.5 % from the beginning of the 4 % loading to the end of 6 % loading. Fig. 14 shows the response curves and variation of mechanical properties for 4 %, 5 %, and 6 % loadings and provides a more precise depiction of the cyclic stability achieved throughout loading. These results suggest that a training protocol of 30 cycles at 6 % strain is satisfactory for achieving cyclic stability under varying amplitude loading for the SMA cable.

Finally, the response of SMA cable at 4 %, 5 %, and 6 % strain loadings are compared for the untrained and trained SMA cables in Fig. 15. All three loading cycles during the first test at each strain amplitude loading are shown in the figure. The data suggests that training the SMA cable reduces the phase transformation stress levels. The lowest phase transformation stress levels are observed for the SMA cable trained at 6 % strain. The decrease in phase transformation stress levels with training can be attributed to the generation of defects or retained martensite during the phase transformation process [49]. As the interface between martensite and austenite forms and moves, defects arise at the boundary due to the lattice mismatch between the two phases, leading to the formation of dislocations. The defects formed during these cycles create internal stresses that favor specific martensite variants and facilitates the transformation of these variants. Consequently, the stresses required to initiate phase transformations are reduced [37–39].

The maximum stress observed during 4 % strain loading is nearly the same for the untrained specimen and the specimen trained at 4 % strain, while the SMA cables trained 5 % and 6 % have a lower maximum stress. During 5 % loading, the SMA cable trained at 6 % has a maximum stress level of 455 MPa, while the other three specimens reach at 496 MPa. On the other hand, at 6 % strain loading, all four specimens have almost the same maximum stress. This can be attributed to the fact that the SMA cables trained at 6 % strain amplitude initiate the phase transformations at a lower stress level, completes the phase transformations earlier, and start exhibiting a post-phase transformation martensitic hardening behavior. Overall, training SMA cables at higher strain amplitudes results in a more stable response at different strain amplitude loadings but such training affects the phase transformation stress levels, which, in return, somewhat modify the shape of the hysteretic curve.

3.2. *Cyclic stability at high strain amplitudes*

The goal of Series II tests is to identify the effects of higher strain amplitudes on the cyclic response and stability of the SMA cable specimens. This series of testing involves two specimens loaded at three cycles at strain amplitudes incrementally increasing from 7 % up to failure, where the test is stopped when the overall strength of the SMA cable drops below 80 % of its maximum stress observed during the test for the protection of the test equipment. Of the specimens assessed, specimen S6 received the training with 30 cycles at 6 % strain, while specimen S5 remained untrained. In Fig. 16, the stress-strain curves for both specimens under increasing strain amplitude loading are presented. The first loading cycle at each strain amplitude loading is shown in the plots for clarity purposes.

A distinct downward shift in the loops and a pronounced post-phase transformation martensitic hardening behavior with increasing strain amplitude loading are observable for both specimens. Fig. 17 shows the variation of upper plateau stress at 3 % and 6 % strain as well as maximum stress of specimen with strain amplitude. Notably, the trained specimen reaches lower stress values at 3 % strain for all loading amplitudes compared with the untrained specimen. However, the difference between two stress values diminishes with increasing loading amplitude, except at 14 % loading.

On the other hand, both specimens achieve very similar stress values at 6 % strain. Up to an 11 % loading amplitude, the trained specimen exhibits slightly higher stress values (up to 2.5 %) at 6 % strain than the untrained specimen. Similarly, the maximum stress of the trained specimens is 2–6 % higher than that of untrained specimen at loading amplitudes from 7 % to 12 %. However, at 14 % strain loading, the untrained specimen reaches a maximum stress of 1259 MPa, while the

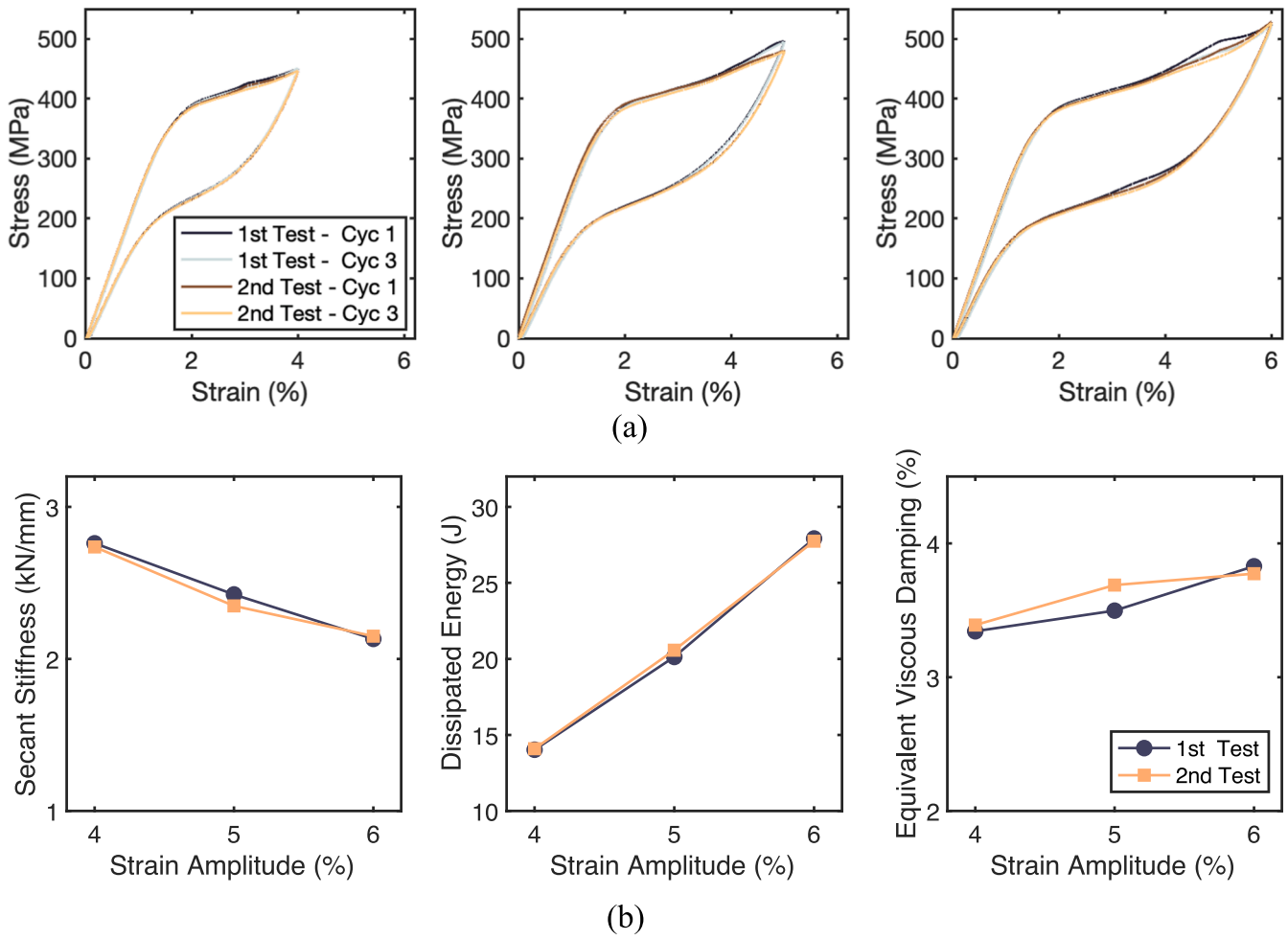

Fig. 11. (a) Hysteresis curves at cycle 1 and cycle 3 for SMA cable trained at 5 % strain and (b) variation of cyclic properties with strain amplitude during 1st and 2nd tests.

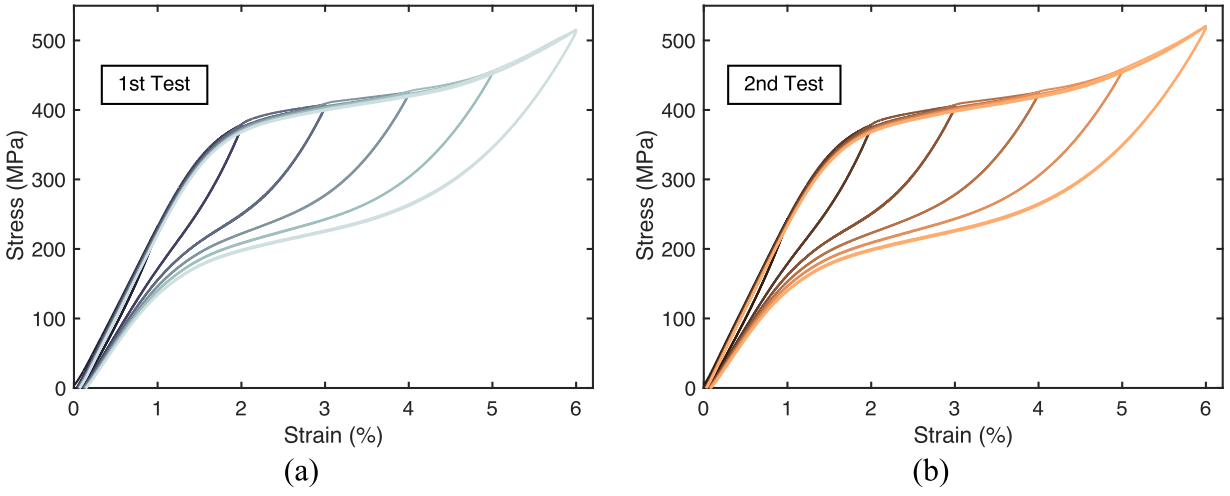

Fig. 12. Stress-strain curves of SMA cable trained at 6 % strain during (a) 1st and (b) 2nd tests.

trained specimen experiences about a 20 % lower maximum stress of 1046 MPa.

Fig. 18 shows the response of the untrained and trained specimens during cycles 1 and 3 at different strain amplitudes. A notable difference in the response of trained and untrained specimens is observed at 7 % and 8 % strain loading, but this difference diminishes as the strain amplitude increases. The response of each specimen becomes almost identical for loading amplitudes between 10 % and 13 %. For 7 % and 8 % loading, the primary difference is observed as a reduced phase transformation start stress level and a steeper phase transformation plateau for the trained specimen.

The identical response above 10 % strain amplitude in both

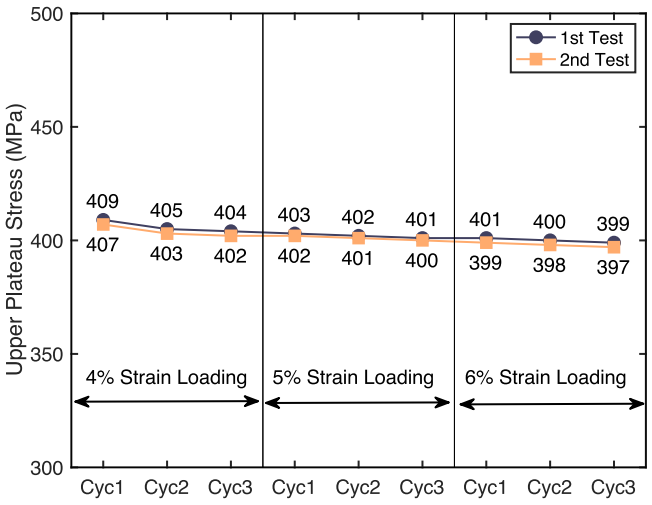

Fig. 13. Variation of UPS for SMA cable trained at 6 % strain during cyclic loading at 4 %, 5 %, and 6 % strain amplitudes.

specimens indicates that training at 6 % loading amplitude does not affect the response at relatively high strain amplitudes. At 13 % loading, both specimens have the same response during the first loading cycle. However, during the third loading cycle, the trained specimen might experience failure at individual wires of the cable, resulting in a sudden drop in stress and leading to lower stress values compared to untrained specimen. Therefore, at 14 % strain loading, the response curves of both specimens differ more, with lower stress values and higher residual strains observed for trained specimen. The trained specimen failed before the third loading cycle, while the untrained specimen failed at the end of the third loading cycle.

When the responses for cycles 1 and 3 at a constant loading amplitude are compared, a more stable response is observed for the trained specimen for the loading amplitudes from 7 % to 10 %. Both trained and untrained specimens exhibit similar degradation in response for 11–13 % strain loadings. As described above, the trained specimen fails earlier than the untrained specimen at 14 % loading.

Fig. 19 shows the variation in mechanical properties of both untrained and trained SMA cables under high strain amplitudes. The figure shows that the secant stiffness is slightly higher in the trained specimen up to 12 % strain. However, the maximum stress (or force) on the trained specimen decreases due to failure of individual wires at 13 % strain loading, which results in an abrupt decrease in the secant stiffness. The dissipated energy in both specimens steadily increases at each strain amplitude, displaying very similar values for the untrained and trained specimens up to 13 % loading. The equivalent viscous damping for the specimens shows a decreasing trend, with slightly higher values for the untrained specimen at lower strain amplitudes. This decrease is attributed to the increasing strain energy in the cable due to strain hardening at higher amplitudes. The total residual strains under increasing displacement amplitude loading of the SMA cable remains below 1 % up

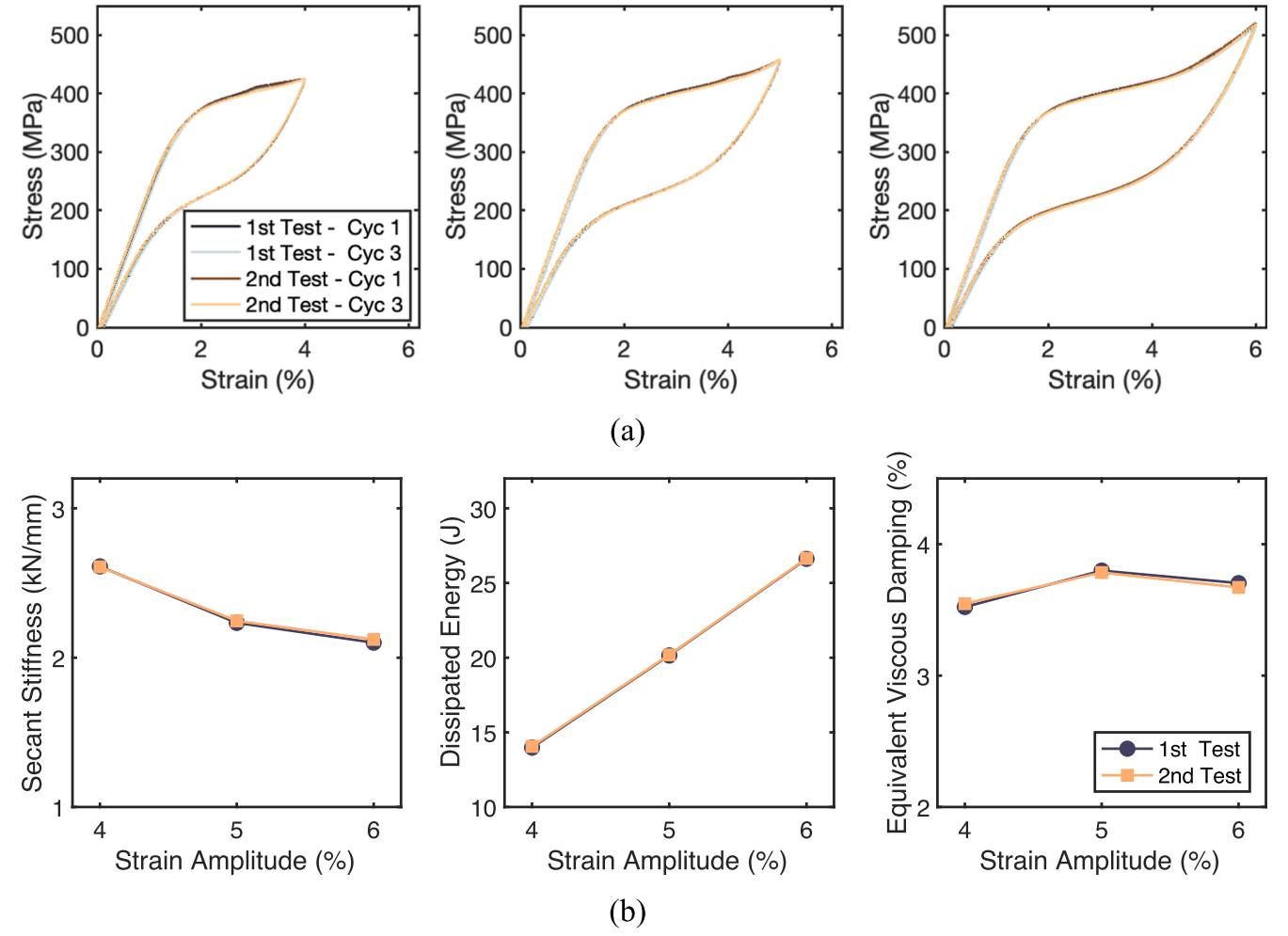

Fig. 14. (a) Hysteresis curves at cycle 1 and cycle 3 for SMA cable trained at 5 % strain and (b) variation of cyclic properties with strain amplitude during 1st and 2nd tests.

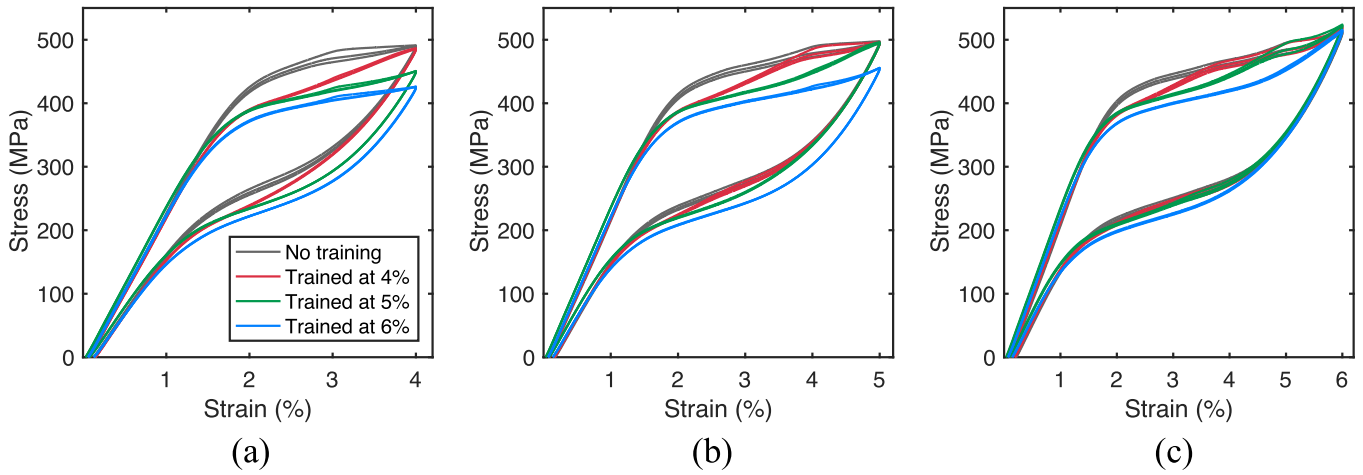

Fig. 15. Comparison of SMA cable response at (a) 4 %, (b) 5 %, and (c) 6 % strain amplitudes for untrained and trained specimens.

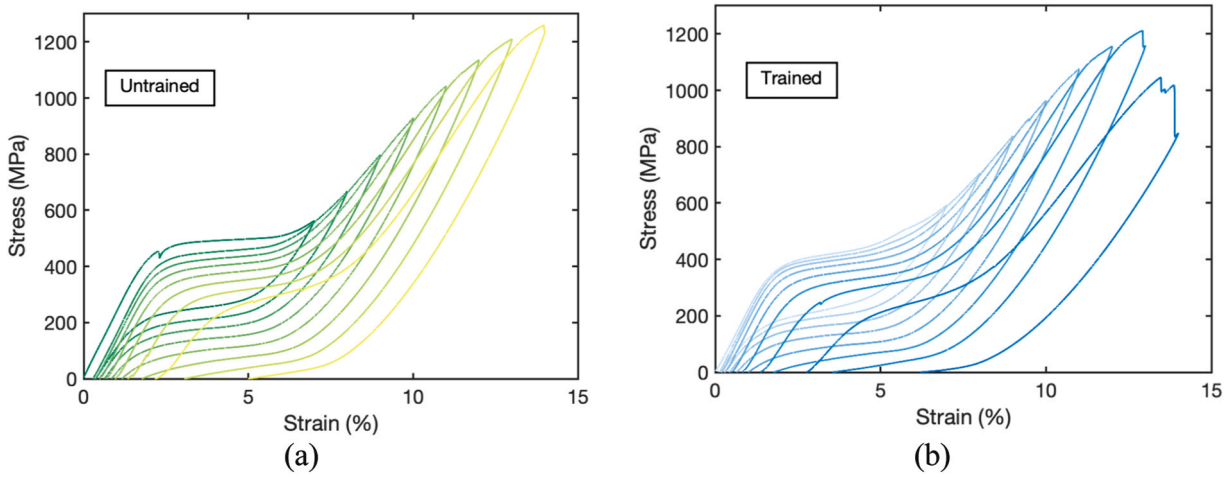

Fig. 16. Stress-strain curve for (a) untrained and (b) trained SMA cables loaded at 7–14 % strain amplitude.

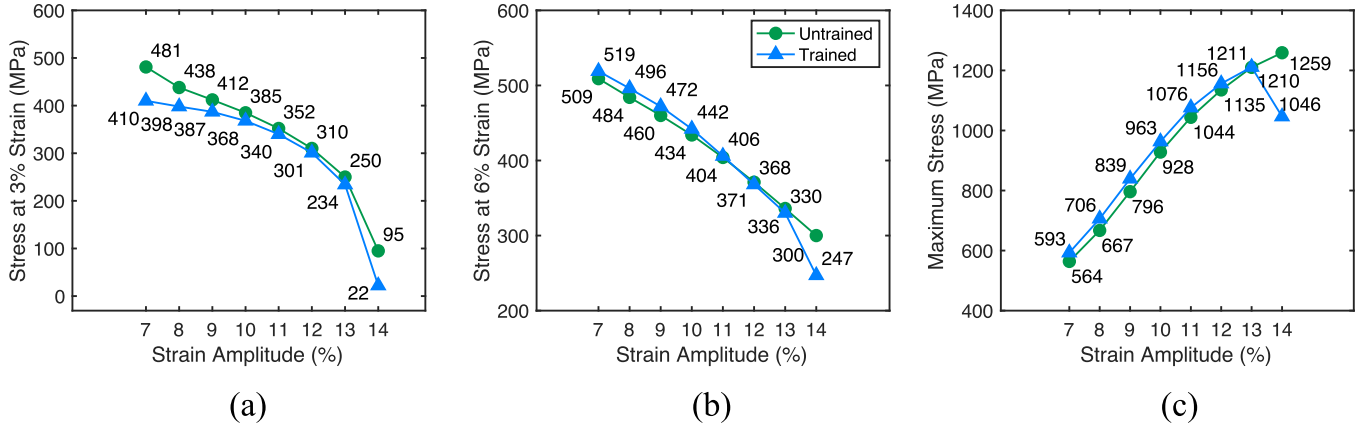

Fig. 17. Variation of stress at (a) 3 % strain, (b) 6 % strain, and (c) maximum stress for untrained and trained SMA cables during 7–14 % strain amplitude loadings.

to 10 % strain loading. Note that the residual strains plotted in Fig. 19 are for the third loading cycle at each strain amplitude. The results reveal that even after undergoing cyclic loading at high strain amplitudes, the accumulated residual strains in the SMA cable remain very small. Higher residual strains occur in the SMA cable when they are loaded beyond 11 % strain. The residual strains in the untrained and trained SMA cable specimens are 3.7 % and 4.3 % after cyclic loading at 13 % strain.

3.3. *Cyclic stability under a low-cycle fatigue loading*

In this section, the cyclic response of the SMA cables under low-cycle fatigue loading at constant strain loading amplitude is examined. The test comprises three specimens subject to 31 cycles at constant strains of

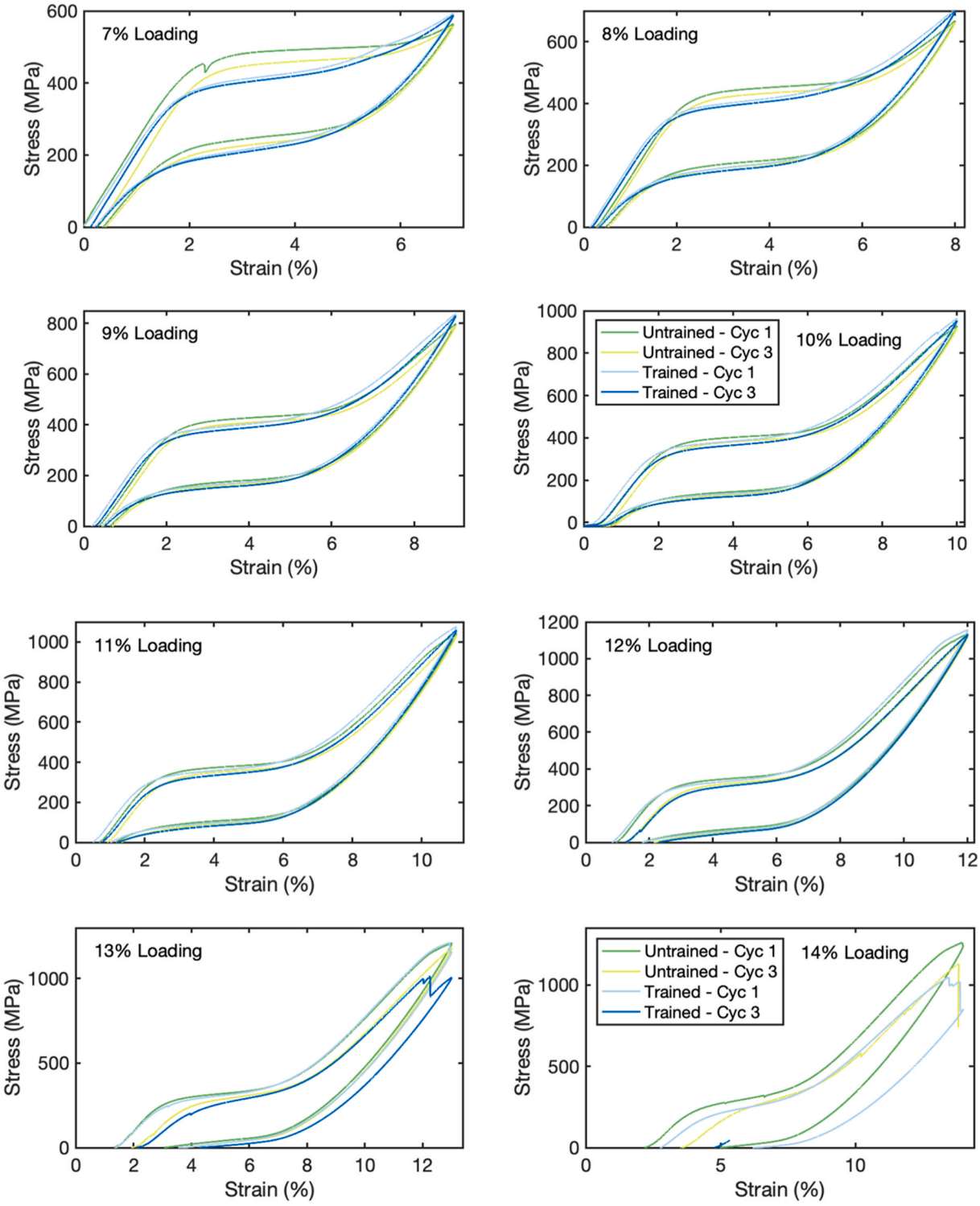

Fig. 18. Hysteresis curves at cycle 1 and cycle 3 for untrained and trained SMA cables loaded at high strain amplitudes.

4 %, 5 %, and 6 %, respectively. Prior to application of prescribed loading, each specimen is trained at 6 % strain for 30 cycles. Fig. 20 shows stress-strain curves obtained from each specimen. The specimens loaded to 4 % and 5 % strain (S7 and S8) exhibit minor degradation between the loading cycles 1 and 3, with the loading curve shifts somewhat downward, while the unloading curve remains almost constant. However, the specimen loaded to 6 % strain (S9) shows a larger cyclic decay between cycles 1 and 31. In this case, both loading and unloading curves shift downward, with the degradation in loading curve being more pronounced. As mentioned earlier, this softening behavior is attributed to the reduction in the stress required to initiate phase transformation, a consequence of the dislocations that arise during cyclic loading [37–39,49].

Fig. 21 shows the variation of the UPS and peak stress with the number of loading cycles for the specimens cyclically loaded at 4 %, 5 %, and 6 %. When the specimen is loaded at 4 % strain for 31 loading cycles, the UPS decreases from 413 MPa at cycle 1–402 MPa at cycle 31, recording a 2.7 % decrease. When the cyclic loading is conducted at 5 %

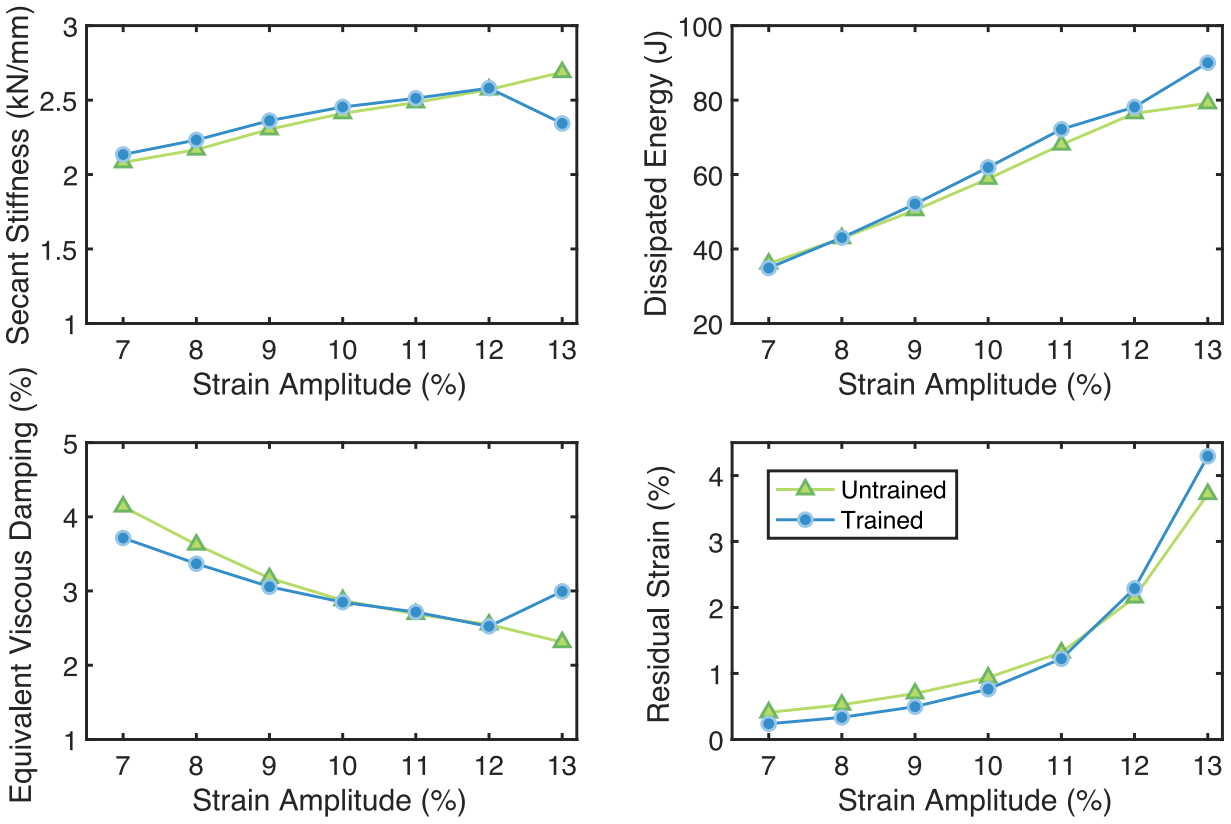

Fig. 19. Variation of cyclic properties computed for untrained and trained SMA cables loaded at higher strain amplitudes.

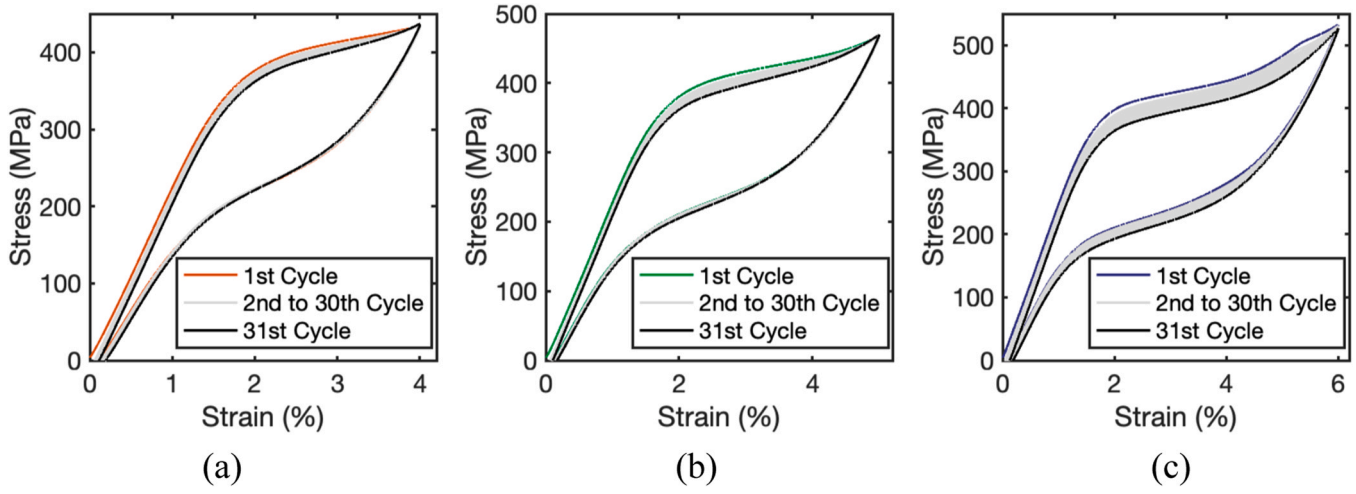

Fig. 20. Stress-strain curves of SMA cable under 30 cyclic loading (a) at 4 % strain, (b) at 5 % strain, and (c) at 6 % strain.

strain, the UPS is 417 MPa at cycle 1, and 398 at cycle 31, indicating a 4.6 % decrease. On the other hand, a 7.3 % decrease in the UPS from 424 MPa at cycle 1–393 MPa at cycle 31 is observed when cyclic loading of the SMA cables is conducted at 6 % strain. Although the upper plateau stress levels experience some decrease with cyclic loading, the peak stress of the specimens during the cyclic loading remains almost constant. In particular, the peak stress during the cyclic loading at 4 % and 5 % increases by 0.4 % and 0.7 %, while the peak stress of the specimen loaded at 6 % strain decreases by 1.1 %.

Fig. 22 displays the variation of mechanical properties computed for the specimens S7 to S9 with the number of loading cycles. The secant stiffness exhibits an almost constant trend with the number of loading cycles for each specimen, as the peak stress does not change considerably during the cyclic loading. The dissipated energy somewhat decreases during the initial loading cycles, but then the rate of this decrease significantly reduces. This decrease in the dissipated energy is due to the fact that upper plateau stress levels shift downward more than the lower plateau stresses, resulting in slightly smaller hysteresis loops. The variation of equivalent viscous damping with number of loading cycles also shows the same trend as the dissipated energy.

3.4. *Effects of displacement history on cyclic response*

The effects of initial loading of SMA cables at high strain amplitudes on their hysteretic response and cyclic stability are studied. To this end, the test contains three specimens (S10, S11, and S12) pre-loaded for

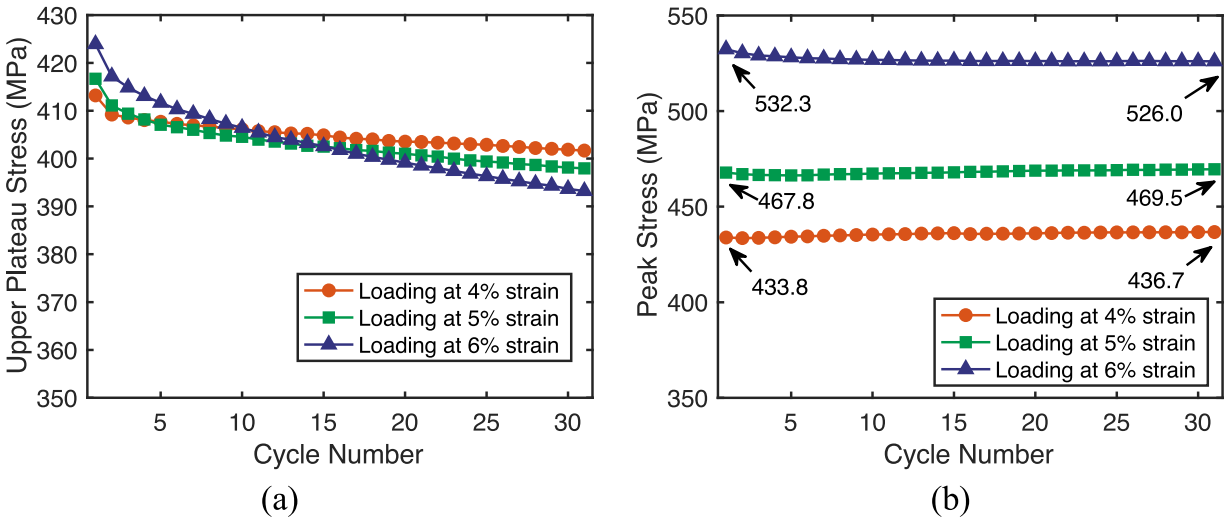

Fig. 21. Variation of (a) UPS and (b) peak stress during cycling loading at 4 %, 5 %, and 6 % strain amplitudes.

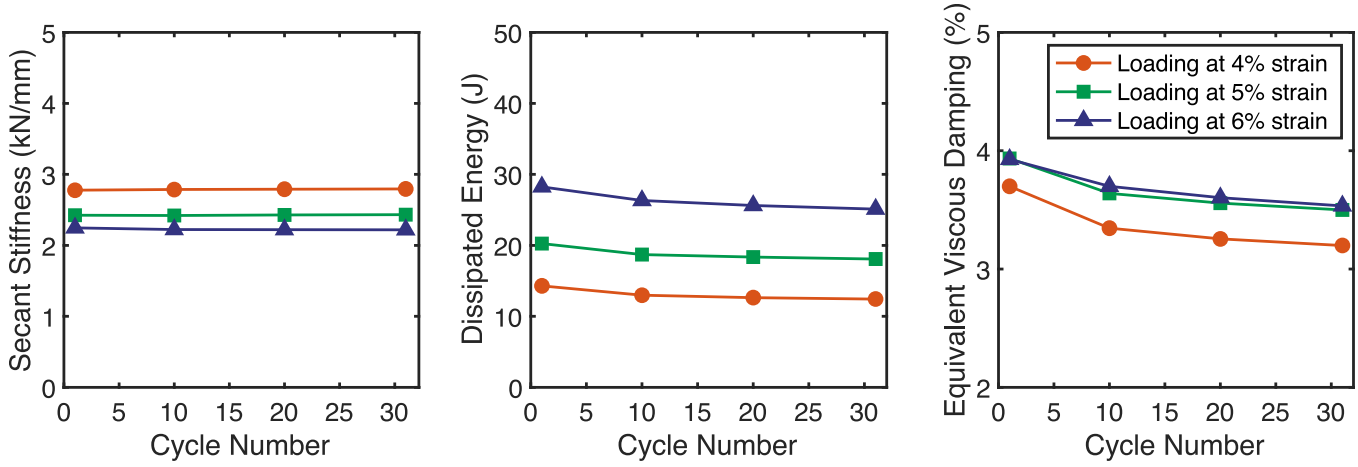

Fig. 22. Variation of mechanical properties of SMA cable during cyclic loading at 4 %, 5 %, and 6 % strain amplitudes.

three cycles at 6 %, 8 % and 10 % strain, respectively, and then tested for three cycles at strain amplitudes from 1 % to 6 %. The cyclic responses of these three specimens are also compared to specimen S1, which can be considered as none pre-loaded specimen. No training cycles are applied to the specimens before pre-loading, as it would skew results and function as additional pre-loading. Fig. 23(a) displays the response of the specimens S10, S11, and S12 under increasing strain amplitude loading. The initial loading cycles are shown in gray in the same plot. Since the specimens are not trained, there is a clear difference between the first loading cycle of initial loading and the other two cycles. Fig. 23(b) compares the first and third loading cycles at 6 % strain for the specimens initially loaded at 6 %, 8 %, and 10 % strain. There is no degradation between the first and third loading cycles regardless of the pre-loading conditions.

Fig. 24 shows the cyclic response comparison for the specimens with various pre-loading conditions for 4 %, 5 %, and 6 % strain loadings. Pre-loading at 8 % or 10 % clearly shifts the hysteresis loops downward. However, no residual strain is introduced due to these large amplitude pre-loadings. A pre-loading at 6 % does not change the forward phase transformation stress level but decreases the slope of the phase transformation plateau and maximum stress at 4 % and 5 % strain loading compared to the specimen without a pre-loading. However, the response of these two specimens becomes almost identical at 6 % loading. On the other hand, an initial loading at 8 % and 10 % decreases the phase transformation stress levels, leading to a lower strength for the specimens with initial high amplitude loading.

To quantify the change in stress levels resulting from pre-loading at high displacement amplitudes, Fig. 25 compares the UPS and peak stress observed in specimens with different initial loading conditions when cyclically loaded from 4 % to 6 % strain. The UPS decreases with cyclic loading for all specimens, with the rate of this decrease being higher for the specimen with no initial loading (S3). However, peak stress remains almost constant at each strain amplitude loading for all specimens.

An initial loading at 6 % strain does not cause significant change in the UPS and peak stress compared to the specimen with no initial loading. However, when the initial loading is higher than 6 %, a more considerable effect of initial loading on these parameters is observed. Specifically, the mean decrease in the UPS for the specimen with 6 % initial loading compared to the specimen without initial loading during the cyclic loading from 4 % to 6 % is only 3 %. In contrast, the same decrease is 7 % and 15 % for the specimens with 8 % and 10 % initial loading, respectively. Similarly, the mean decrease in the peak stress during the cyclic loading from 4 % to 6 % for the specimens initially loaded at 6 %, 8 %, and 10 % are 2 %, 7 %, and 13 % compared to the specimen without initial loading.

Fig. 26 displays the variation in mechanical properties computed for the specimens with different initial loading conditions. Pre-loading at larger strain amplitudes leads to a decrease in secant stiffness, as the

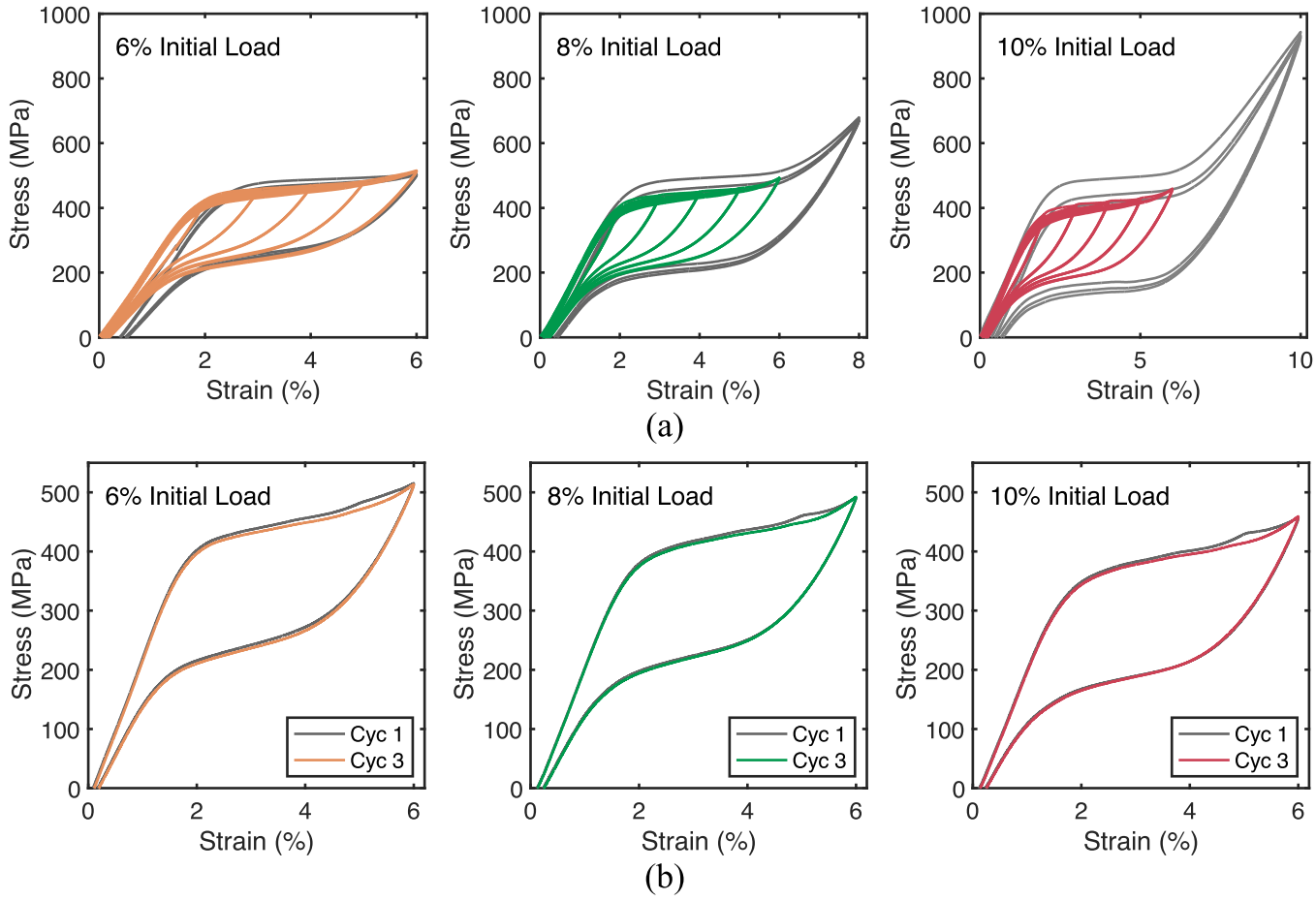

Fig. 23. (a) Stress-strain curves of SMA cable specimens initially loaded at 6 %, 8 %, and %10 strain, (b) Hysteresis curves at cycle 1 and cycle 3 at 6 % strain for each specimen.

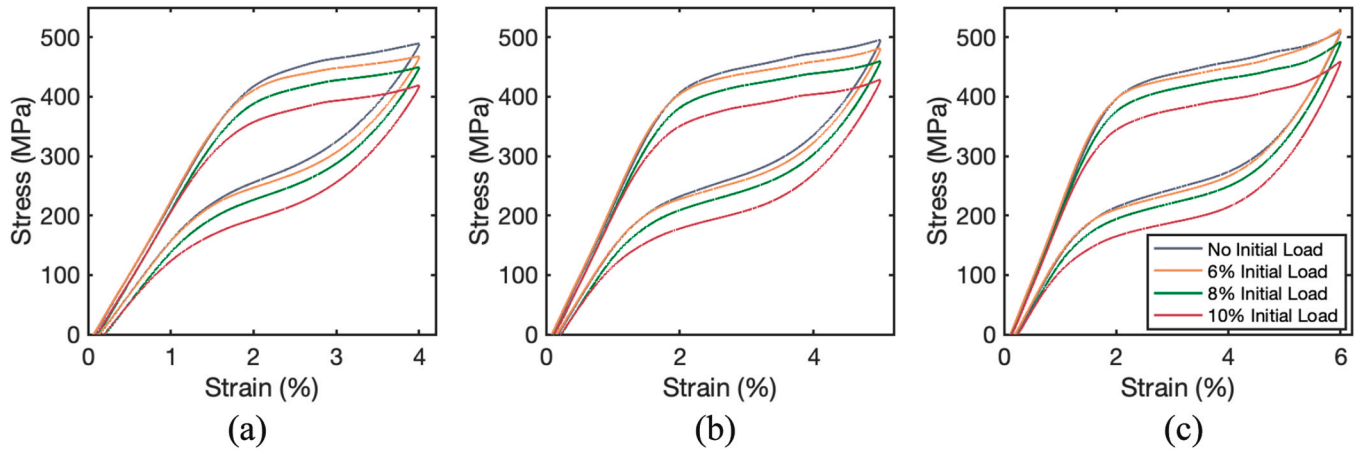

Fig. 24. Comparison of SMA cable response at (a) 4 %, (b) 5 %, and (c) 6 % strain loading for specimens with various initial loading conditions.

peak stress decreases with pre-loading. The dissipated energy shows a near identical response for all four specimens, indicating no effect of pre-loading on the amount of dissipated energy. This is because both upper and lower plateau stresses shift downward with increasing amplitude pre-loading, leading to similar hysteresis loops. The equivalent viscous damping follows a trend opposite to the secant stiffness where the equivalent viscous damping increases as the pre-loading strain amplitude increases. This increase in the equivalent viscous damping is due to the fact that the stored elastic energy is smaller for the specimens with high initial loading.

3.5. *Prestrain effects on cyclic stability*

The final series of testing explores how applying prestrain to the SMA cable specimens affects cyclic response and stability of the specimens. The test includes two specimens prestrained at 1 % and 2 % strain, respectively. Each specimen undergoes training for 30 cycles at 6 % strain before the testing. The testing consists of three loading cycles at

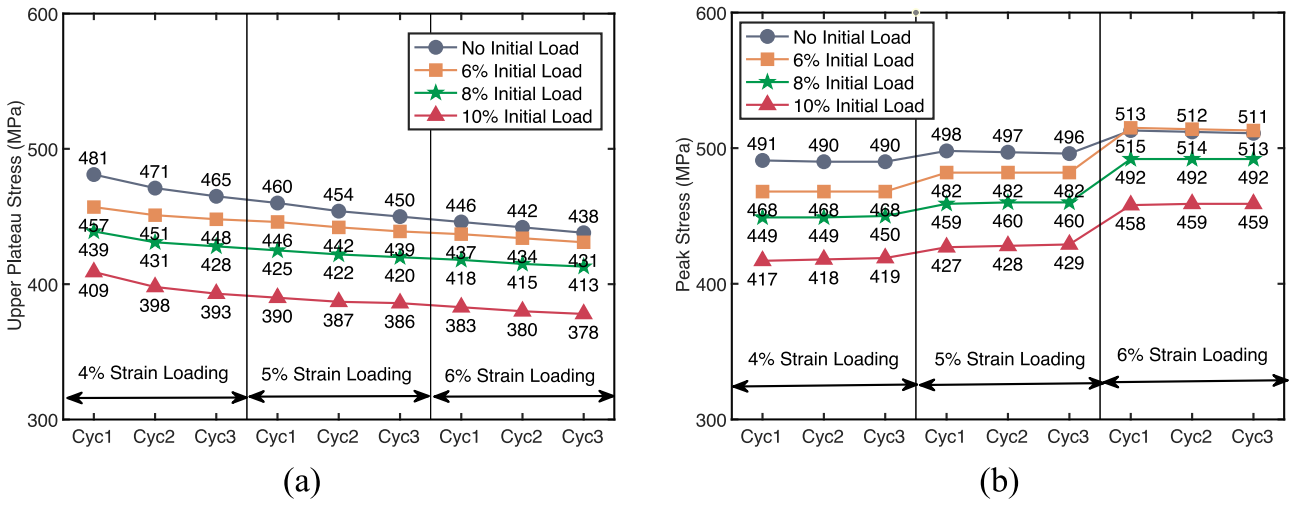

Fig. 25. Variation of (a) UPS and (b) peak stress during cycling loading at 4 %, 5 %, and 6 % strain amplitudes for specimens with various initial loading conditions.

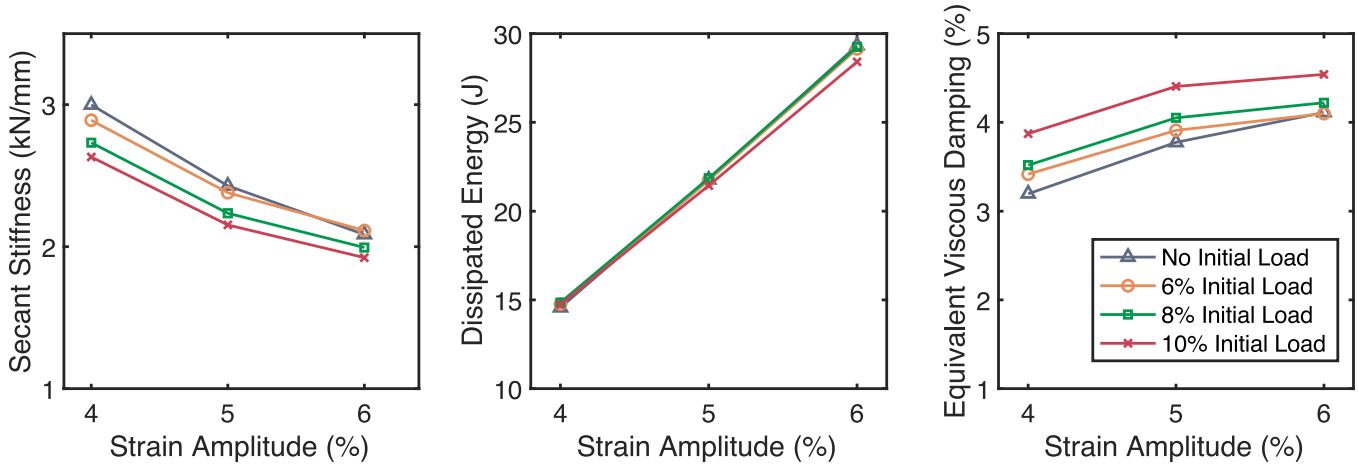

Fig. 26. Variation of cyclic properties computed for specimens with various initial loading conditions.

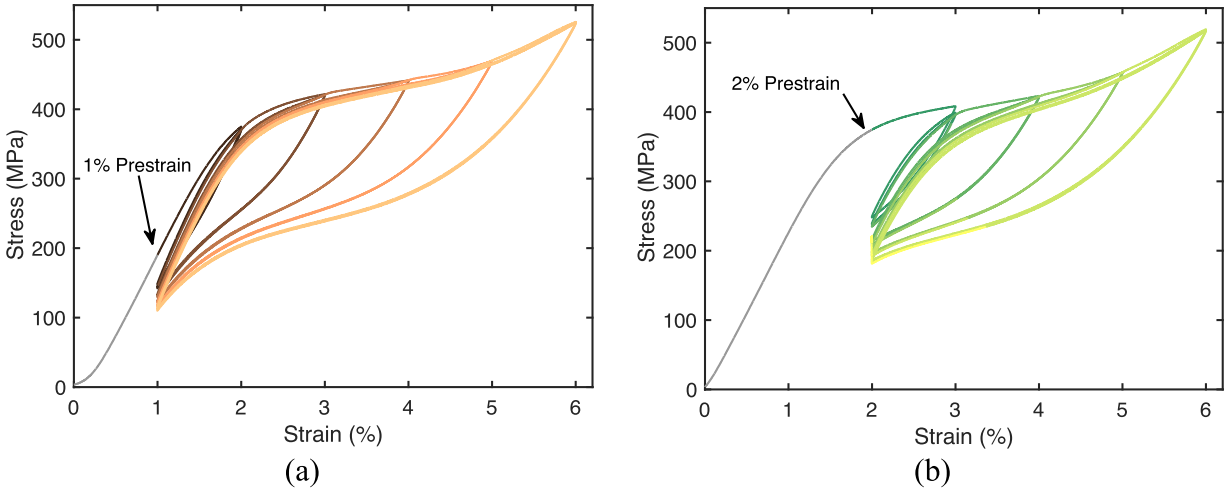

Fig. 27. Stress-strain curves of SMA cable with (a) 1 % prestrain and (b) 2 % prestrain.

incrementally increasing strain amplitudes from 1 % to 6 %. The same loading protocol is repeated after one hour. Fig. 27 shows the stress-strain curves of SMA cable under increasing strain amplitude loading during the initial testing. All three loading cycle response at each strain amplitude are plotted in the figure.

Fig. 28(a) compares the response of the SMA cable with 1 % prestrain and 2 % prestrain when loaded at 6 % strain. These results are also compared with those of specimen S4, which is trained and loaded in the

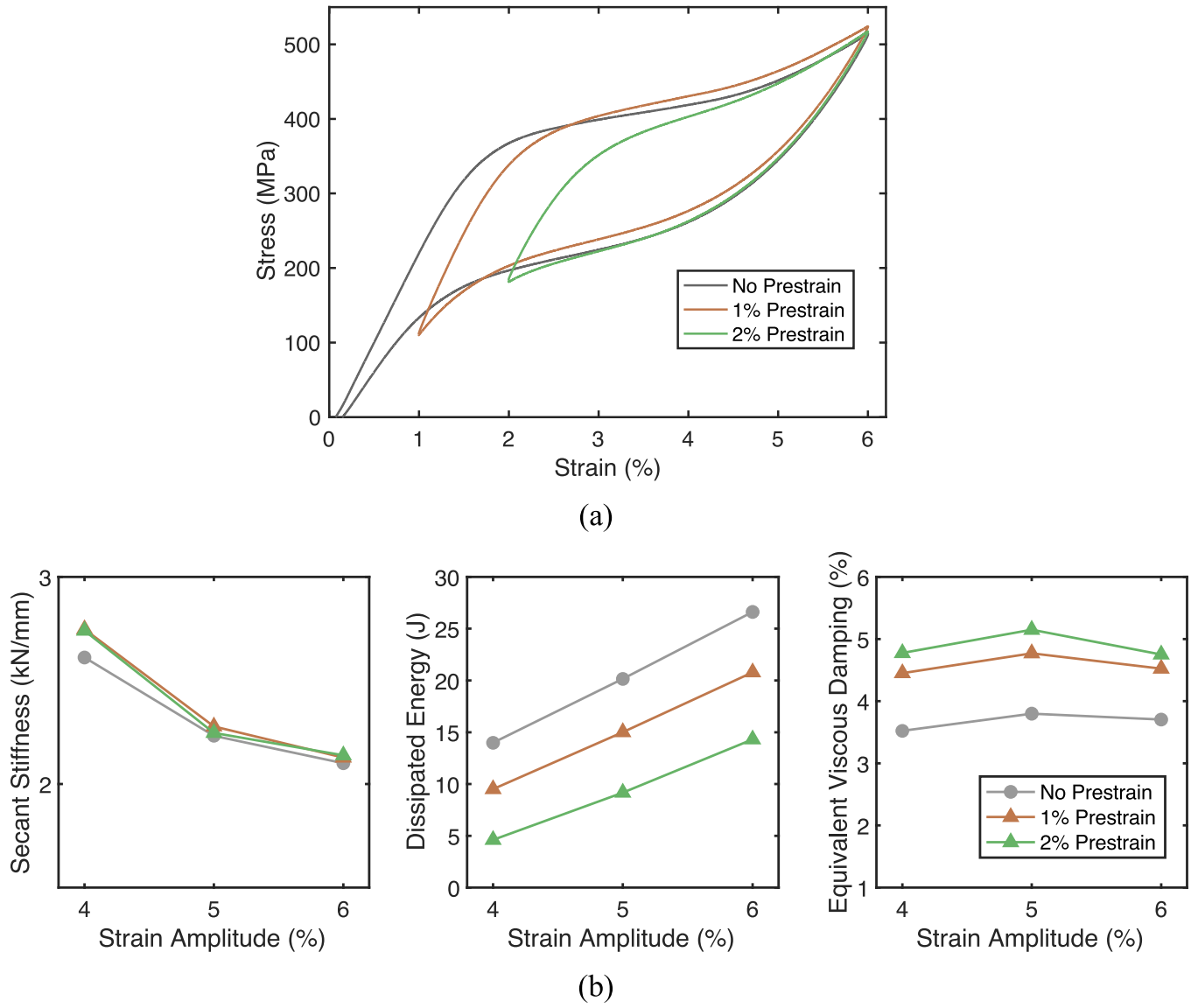

Fig. 28. (a) Comparison of SMA cable response at 6 % strain loading and (b) variation of mechanical properties with strain amplitude for specimens with no prestrain, 1 % prestrain and 2 % prestrain.

same way but has no prestrain. Fig. 28(b) shows the mechanical properties computed for the specimens with no prestrain, 1 % prestrain, and 2 % prestrain at different strain amplitude loadings. The secant stiffness is almost identical between the three specimens, especially as loading approaches 6 % strain. It can be observed that dissipated energy decreases with the applied prestrain. This can be attributed to the less area under the cyclic loops for specimens that have been prestrained. On the other hand, the mean equivalent viscous damping for 4 %, 5 %, and 6 % strain amplitude loadings are 3.7 %, 4.6 %, and 4.9 %, respectively for specimens with no prestrain, 1 % prestrain, and 2 % prestrain. The observed higher damping ratios with applied prestrain can be attributed to smaller stored energies in equivalent linear systems when the prestrain is present.

Finally, Fig. 29 compares the response of SMA cables with the applied prestrain at cycles 1 and 3 during first test and cycle 3 at different strain amplitude loadings during second test to examine any cyclic degradation. It can be seen that the specimen with 1 % prestrain exhibits a stable and repeatable response when loaded at 4 % strain or above, but there is a somewhat variation in the response of the specimen with 2 % prestrain at different loading cycles when they are loaded at lower strain amplitudes. In particular, relatively higher stress values during the cycle 1 of first test are observed during especially 4 % strain amplitude loading.

4. Conclusions

This paper presents a comprehensive characterization study of shape memory alloy cables, focusing on the influence of different variables on the cyclic response and stability of the cable. Cyclic tensile tests are conducted on fourteen SMA cable specimens, addressing various objectives including identifying an optimal training protocol, assessing low-cycle fatigue performance, and exploring the effects of displacement history and prestrain. Various cyclic properties are computed and analyzed based on test objectives. The following conclusions can be drawn from the testing conducted in this study:

- SMA cables exhibit softening behavior under cyclic loading. However, the extent of this softening remains limited, even for untrained specimens. Specifically, the upper plateau stress decreases by 9 % after undergoing three cycles at 4 %, 5 %, and 6 % strain for the untrained specimen.

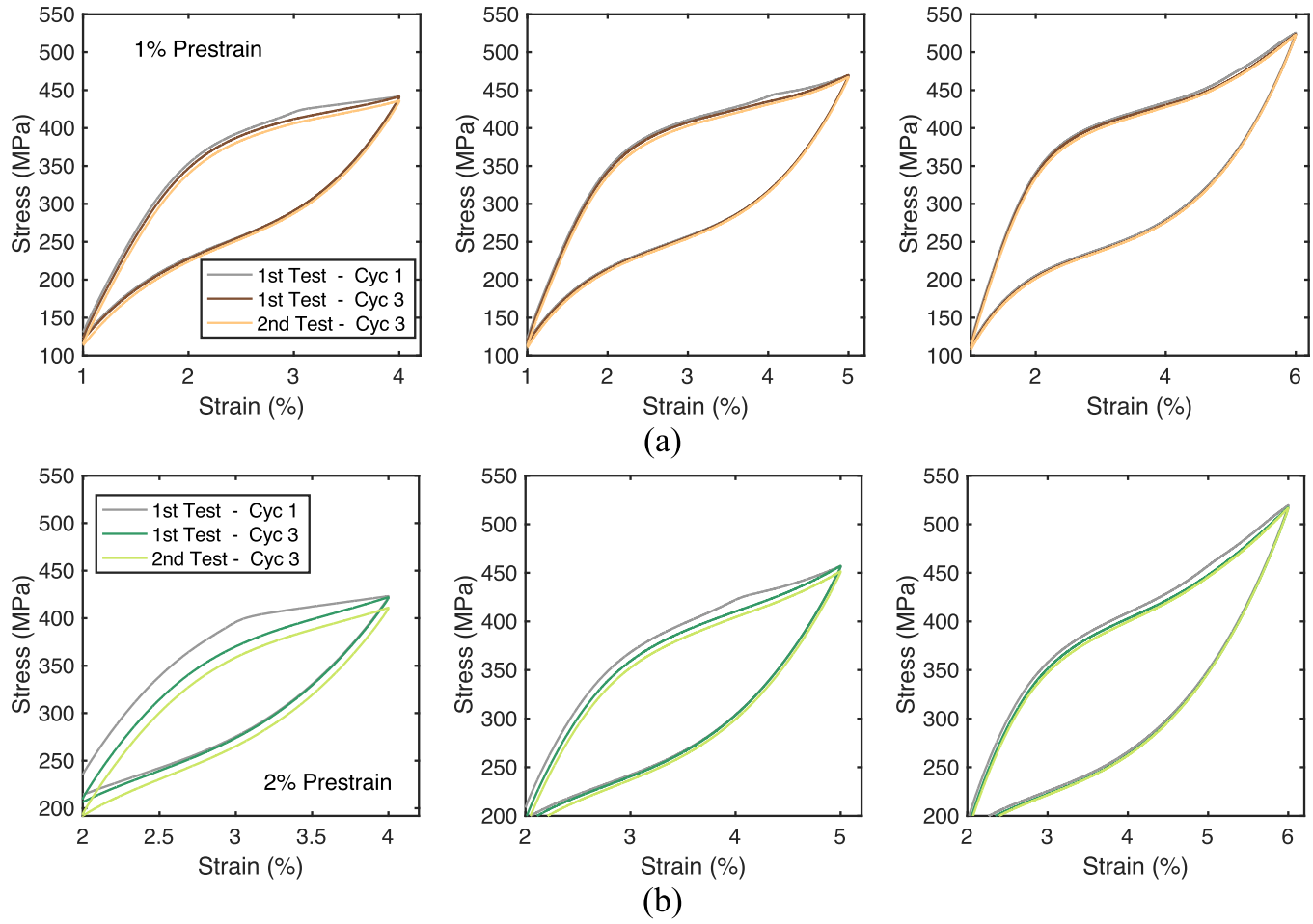

Fig. 29. Hysteresis curves at cycles 1 and 3 during 1st test and cycle 3 during 2nd test at different strain amplitude loadings for SMA cable with (a) 1 % prestrain and (b) 2 % prestrain.

- In comparison to untrained specimens, the SMA cables that underwent training loading exhibit more stable cyclic response when subjected to the same loading protocol twice.
- Training SMA cables at a strain amplitude within their superelastic strain range results in the stabilization of SMA behavior up to the training strain amplitude, but variations are still observed at higher strain amplitude loadings.
- The application of training loading cycles reduces transformation stress levels. Therefore, the trained SMA cables have shown lower upper plateau stress levels. However, the peak stress at training strain amplitude (i.e. 6 % strain) loading is observed to be almost the same for both untrained and trained SMA cables.
- During the increasing strain amplitude loading at high strain amplitudes (7–14 %), the trained and untrained specimens have exhibited similar response beyond 8 % loading. This indicates that when the untrained SMA cable is subjected to a few large amplitude loadings, its response gets mostly stabilized. Nevertheless, the trained SMA cable failed earlier than the untrained SMA cable.
- When an SMA cable, trained at 6 % strain for 30 cycles, undergoes low-cycle fatigue loading at 4 %, 5 %, and 6 %, there is very limited cyclic softening in the response. Specifically, the upper plateau stress experiences a maximum decrease of 4.6 %, while the peak stress shows a maximum reduction of 1.1 % for the tests conducted at different strain amplitudes.
- When an untrained SMA cable is initially loaded at a certain strain amplitude, this causes softening in subsequent cyclic loading within its superelastic range. Specifically, when subjected to an initial loading of 10 % strain, the SMA cable exhibits a 15 % decrease in upper plateau stress and a 13 % decrease in peak stress. These decreases diminish when the initial loading is reduced to either 8 % or 6 %.
- Applying 1 % or 2 % prestrain to SMA cables causes phase transformations to occur at lower stress levels compared to untrained cables. However, the peak stress at 6 % loading, as well as the reverse plateau stress level, does not change considerably. Consequently, smaller hysteresis loops, i.e., dissipated energy, are observed for cables with prestrain. In contrast, they exhibit higher equivalent viscous damping due to their smaller stored elastic energy.

Based on these findings, a few recommendations can be made for researchers and practitioners working with SMA cable-based seismic protection technologies. First, it is highly recommended to apply a training loading protocol to SMA cables prior to their implementation. This will help to establish a stable and consistent cable response from which critical design parameters such as yield force, post-yield hardening behavior and failure strength can be obtained. The training strain applied to the SMA cables is suggested to be at least the maximum strain induced in an SMA-based device during a design-level earthquake. Once trained, it is expected that SMAs will exhibit a stable response during an earthquake loading where they generally are strained at high strain amplitudes only a few cycles. Furthermore, applying a low level of prestrain (about %1) will increase the stiffness of such SMA-based devices and slightly improve the equivalent viscous damping. The results of cyclic loading tests on pre-strained SMA cables indicate that a stable response can be expected on such pre-tensioned SMA cables.

CRediT authorship contribution statement

Malik Corum: Methodology, Investigation, Formal analysis, Data curation. **Osman Ozbulut:** Writing – review & editing, Writing – original draft, Supervision, Resources, Methodology, Funding acquisition, Formal analysis, Conceptualization. **Fei Shi:** Writing – review & editing, Resources, Methodology, Investigation, Funding acquisition, Formal analysis, Data curation.

Declaration of Competing Interest

The authors declare that they have no known competing financial interests or personal relationships that could have appeared to influence the work reported in this paper.

Data Availability

Data will be made available on request.

Acknowledgements

This study is funded by the Natural Science Foundation of China (52208472; 52361135808), the Guangdong Basic and Applied Basic Research Foundation (2021A1515110357; 2023A1515011877), Bureau of Education of Guangzhou Municipality (202255464), as well as National Science Foundation (NSF) under Award No. CMMI-2141073. The opinions expressed in this paper are those of the authors and do not necessarily reflect the views of the sponsors.

References

[1] O.E. Ozbulut, S. Hurlebaus, R. DesRoches, Seismic response control using shape memory alloys: a review, J. Intell. Mater. Syst. Struct. *22* (14) (2011) 1531–1549.
[2] J.C. Wilson, M.J. Wesolowsky, Shape memory alloys for seismic response modification: a state-of-the-art review, Earthq. Spectra *21* (2) (2005) 569–601.
[3] A. Tabrizikahou, M. Kuczma, M. Łasecka-Plura, E.N. Farsangi, M. Noori, P. Gardoni, S. Li, Application and modelling of shape-memory alloys for structural vibration control: state-of-the-art review, Constr. Build. Mater. *342* (2022) 127975.
[4] M.S. Speicher, R. DesRoches, R.T. Leon, Investigation of an articulated quadrilateral bracing system utilizing shape memory alloys, J. Constr. Steel Res. *130* (2017) 65–78.
[5] S. Hu, M.S. Alam, Y. Zhang, Z. Ding, X. He, Partially self-centering braces with NiTi-and Fe-SMA U-shaped dampers, Thin-Walled Struct. (2024) 111605.
[6] F. Shi, Z. Lin, Q. Li, O.E. Ozbulut, Z. He, Y. Zhou, Design, manufacturing, and testing of a hybrid self-centering brace for seismic resilience of buildings, Earthq. Eng. Struct. Dyn. *52* (5) (2023) 1381–1402.
[7] Z.P. Chen, S. Zhu, H. Yu, B. Wang, Development of novel SMA-based D-type self-centering eccentrically braced frames, Eng. Struct. *260* (2022) 114228.
[8] F. Shi, O.E. Ozbulut, Y. Zhou, Influence of shape memory alloy brace design parameters on seismic performance of self-centering steel frame buildings, Struct. Control Health Monit. *27* (1) (2020) e2462.
[9] F. Shi, G. Saygili, O.E. Ozbulut, Y. Zhou, Risk-based mainshock-aftershock performance assessment of SMA braced steel frames, Eng. Struct. *212* (2020) 110506.
[10] C. Qiu, X. Zhao, S. Zhu, Seismic upgrading of multistory steel moment-resisting frames by installing shape memory alloy braces: design method and performance evaluation, Struct. Control Health Monit. *27* (9) (2020) e2596.
[11] A.M. Asfaw, O.E. Ozbulut, Characterization of shape memory alloy energy dissipators for earthquake-resilient structures, Struct. Control Health Monit. *28* (4) (2021) e2697.
[12] A.M. Asfaw, L. Cao, O.E. Ozbulut, J. Ricles, Development of a shape memory alloy-based friction damper and its experimental characterization considering rate and temperature effects, Eng. Struct. *273* (2022) 115101.
[13] W. Wang, C. Fang, A. Zhang, X. Liu, Manufacturing and performance of a novel self-centring damper with shape memory alloy ring springs for seismic resilience, Struct. Control Health Monit. *26* (5) (2019) e2337.
[14] Y. Ping, C. Fang, F. Shi, H. Wu, M.C. Yam, Y. Chen, Experimental and numerical studies on SMA-viscoelastic hybrid self-centering braces. *Smart*, Mater. Struct. *31* (9) (2022) 095048.
[15] H. Qian, H. Li, G. Song, W. Guo, Recentering shape memory alloy passive damper for structural vibration control, Math. Probl. Eng. *2013* (2013) 1–13.
[16] B. Wang, S. Zhu, Cyclic tension–compression behavior of superelastic shape memory alloy bars with buckling-restrained devices, Constr. Build. Mater. *186* (2018) 103–113.
[17] S. Li, F.H. Dezfuli, M.S. Alam, J.Q. Wang, Design, manufacturing, and performance evaluation of a novel smart roller bearing equipped with shape memory alloy wires, Smart Mater. Struct. *31* (2) (2022) 025032.
[18] O.E. Ozbulut, S. Hurlebaus, Energy-balance assessment of shape memory alloy-based seismic isolation devices, Smart Struct. Syst. *8* (4) (2011) 399–412.
[19] F.H. Dezfuli, M.S. Alam, Hysteresis model of shape memory alloy wire-based laminated rubber bearing under compression and unidirectional shear loadings, Smart Mater. Struct. *24* (6) (2015) 065022.
[20] Z. Peng, W. Wei, L. Yibo, H. Miao, Cyclic behavior of an adaptive seismic isolation system combining a double friction pendulum bearing and shape memory alloy cables, Smart Mater. Struct. *30* (7) (2021) 075003.
[21] B. Wang, S. Zhu, F. Casciati, Experimental study of novel self-centering seismic base isolators incorporating superelastic shape memory alloys, J. Struct. Eng. *146* (7) (2020) 04020129.
[22] S. Cao, O.E. Ozbulut, F. Shi, J. Deng, Experimental and numerical investigations on hysteretic response of a multi-level SMA/lead rubber bearing seismic isolation system. *Smart*, Mater. Struct. *31* (3) (2022) 035024.
[23] J. Deng, F. Hu, O.E. Ozbulut, S. Cao, Verification of multi-level SMA/lead rubber bearing isolation system for seismic protection of bridges, Soil Dyn. Earthq. Eng. *161* (2022) 107380.
[24] S. Cao, O.E. Ozbulut, F. Shi, J. Deng, An SMA cable-based negative stiffness seismic isolator: development, experimental characterization, and numerical modeling, J. Intell. Mater. Syst. Struct. *33* (14) (2022) 1819–1833.
[25] X. Yang, H. Zhou, X. Yang, X. Zhou, S.Y. Zhang, Y. Du, Shape memory alloy strands as cross-ties: Fatigue behavior and model-cable net tests, Eng. Struct. 245 (2021) 112828.
[26] M. Lian, Y. Zhou, Y. Wang, M. Su, Experimental investigation of mechanical properties of NiTi superelastic shape memory alloy cables, J. Constr. Steel Res. 214 (2024) 108447.
[27] Y. Shi, H. Qian, L. Kang, Z. Li, L. Xia, Cyclic behavior of superelastic SMA cable and its application in an innovative self-centering BRB. Smart, Mater. Struct. 30 (9) (2021) 095019.
[28] M.M. Sherif, O.E. Ozbulut, Thermomechanical and electrical response of a superelastic NiTi shape memory alloy cable, J. Intell. Mater. Syst. Struct. 31 (19) (2020) 2229–2242.
[29] H. Qian, D. Wei, Y. Shi, Z. Li, H. Li, Pre-tensioned SMA cable tests and its application in a novel self-centering viscoelastic damper, Soil Dyn. Earthq. Eng. 168 (2023) 107850.
[30] H. Qian, C. Fan, Y. Shi, J. Xu, Z. Li, E. Deng, Development and investigation of an innovative shape memory alloy cable-controlled self-centering viscoelastic coupling beam damper for seismic mitigation in coupled shear wall structures, Earthq. Eng. Struct. Dyn. 52 (2) (2023) 370–393.
[31] R. DesRoches, J. McCormick, M. Delemont, Cyclic properties of superelastic shape memory alloy wires and bars, J. Struct. Eng. *130* (1) (2004) 38–46.
[32] H. Soul, A. Isalgué, A. Yawny, V. Torra, F. Lovey, Pseudoelastic fatigue of NiTi wires: frequency and size effects on damping capacity, Smart Mater. Struct. 19 (8) (2010) 085006, https://doi.org/10.1088/0964-1726/19/8/085006.
[33] F. Shi, O.E. Ozbulut, Z. Li, Z. Wu, F. Ren, Y. Zhou, Effects of ambient temperature on cyclic response and functional fatigue of shape memory alloy cables, J. Build. Eng. *52* (2022) 104340.
[34] O.E. Ozbulut, S.M. Daghash, M.M. Sherif, Shape memory alloy cables for structural applications, J. Mater. Civ. Eng. 28 (2016) 4.
[35] S. Miyazaki, T. Imai, Y. Igo, K. Otsuka, Effect of cyclic deformation on the pseudoelasticity characteristics of Ti-Ni alloys, Metall. Trans. 17 (1) (1986) 115–120.
[36] D. Wolons, F. Gandhi, B. Malovrh, Experimental investigation of the pseudoelastic hysteresis damping characteristics of shape memory alloy wires, J. Intell. Mater. Syst. Struct. 9 (2) (1998) 116–126.
[37] F. Furgiuele, P. Magarò, C. Maletta, E. Sgambitterra, Functional and structural fatigue of pseudoelastic NiTi: global vs local thermo-mechanical response, Shape Mem. Superelasticity *6* (2020) 242–255.
[38] K. Nargatti, S. Ahankari, Advances in enhancing structural and functional fatigue resistance of superelastic NiTi shape memory alloy: a Review, J. Intell. Mater. Syst. Struct. *33* (4) (2022) 503–531.
[39] W.S. Ko, W.S. Choi, G. Xu, P.P. Choi, Y. Ikeda, B. Grabowski, Dissecting functional degradation in NiTi shape memory alloys containing amorphous regions via atomistic simulations, Acta Mater. 202 (2021) 331–349.
[40] X. Ran, K. Ke, Y. Shi, H. Li, 0.8 mm Ni–Ti shape memory alloy wires: Post-training behavior and application in a cold-formed steel structure, Structures 56 (2023) 104812.
[41] D. Davarnia, S. Cheng, N. Van Engelen, Effect of training on the cyclic behaviour of SMA wire, Smart Mater. Struct. *32* (8) (2023) 085013.
[42] Y. Xia, H. Zhou, X. Yang, X. Zhou, S.Y. Zhang, Y. Du, Shape memory alloy strands as cross-ties: Fatigue behavior and model-cable net tests, Eng. Struct. 245 (2021) 112828.
[43] Y. Zhang, Z. Moumni, J. Zhu, W. Zhang, Effect of the amplitude of the training stress on the fatigue lifetime of NiTi shape memory alloys, Scr. Mater. 149 (2018) 66–69.
[44] McCormick, J., Barbero, L., & DesRoches, R. (2005). Effect of mechanical training on the properties of superelastic shape memory alloys for seismic applications. Proceedings of SPIE.
[45] M. Dolce, D. Cardone, Mechanical behaviour of shape memory alloys for seismic applications 1. Martensite and austenite NiTi bars subjected to torsion, Int. J. Mech. Sci. 43 (11) (2001) 2631–2656.
[46] P. Lafortune, J. McCormick, R. DesRoches, P. Terriault, Testing of superelastic recentering pre-strained braces for seismic resistant design, J. Earthq. Eng. 11 (3) (2007) 383–399.

[47] Y. Zhang, S. Zhu, Seismic response control of building structures with superelastic shape memory alloy wire dampers, J. Eng. Mech. *134* (3) (2008) 240–251.
[48] F. Shi, Y. Zhou, O.E. Ozbulut, S. Cao, Development and experimental validation of anchorage systems for shape memory alloy cables, Eng. Struct. *228* (2021) 111611.
[49] Y. Zhang, X. Chai, X. Ju, Y. You, S. Zhang, L. Zheng, W. Zhang, Concentration of transformation-induced plasticity in pseudoelastic NiTi shape memory alloys: Insight from austenite–martensite interface instability, Int. J. Plast. *160* (2023) 103481.